

Classification of Fullerene Isomers from C₄₀ to C₄₈

Alexander I. Melker^{1,*}, Aleksandra N. Matvienko², Maria A. Krupina³

¹ St. Petersburg Academy of Sciences on Strength Problems, Peter the Great St. Petersburg Polytechnic University, Polytekhnicheskaya 29, 195251, St. Petersburg, Russian Federation

² Department of Mechanics and Control Processes, Peter the Great St. Petersburg Polytechnic University, Polytekhnicheskaya 29, 195251, St. Petersburg, Russian Federation

³ Department of Physics, Peter the Great St. Petersburg Polytechnic University, Polytekhnicheskaya 29, 195251, St. Petersburg, Russian Federation

Article history

Received April 25, 2022
Accepted May 29, 2022
Available online June 30, 2022

Abstract

We have designed possible structures of the isomers of midi-fullerenes, namely C₄₀, C₄₂, C₄₄, C₄₆, and C₄₈; three the most natural mechanisms of their formation being used: fusion of carbon cupolas having the same symmetry; fusion of fullerenes having compatible symmetry and embedding carbon dimers into initial fullerenes. The energies of the fullerenes calculated through the use of molecular mechanics are presented together with their graphs. It is found that in the majority of cases the minimum-energy fullerenes are those, which have tetrahedral symmetries. The maximum-energy fullerenes refer to the three-fold T-symmetry.

Keywords: Isomer; Fullerene; Graph; Growth; Symmetry

1. INTRODUCTION

The periodic system of fullerenes predicts their symmetry as well as the existence of their isomers having different symmetry [1,2]. The isomers can be got by different mechanisms. In Ref. [3] we have classified the natural mechanisms of obtaining new fullerenes, namely: embedding a carbon dimer into an initial fullerene, fusion of the carbon cupolas having the same symmetry and fusion of the fullerenes having compatible symmetry.

In this contribution we present the classification of fullerene isomers, give their structure and energy in the range from C₄₀ to C₄₈ which can be produced through the use of these mechanisms. We will give the structure of the fullerenes for two extreme electronic configurations: with single bonds only and with single and double ones, the maximum number of possible double bonds being positioned symmetrically.

2. PERFECT BASIC AND IMPERFECT INTERMEDIATE FULLERENES

According to the periodic system of fullerenes, there are two main types of fullerenes; the perfect basic ones and imperfect intermediate ones. The perfect basic fullerenes have ideal structure and ordinary symmetry. The imperfect intermediate fullerenes have extra carbon dimers. By analogy with crystal physics, we have assumed [1] that these extra dimers play the role of defects which violate the symmetry and create local imperfections. However, for defect crystals the long-range order is observed experimentally. In order to underline this peculiarity, such long-range order is referred to as the topological long-range one [4]. Using analogous terminology, we have defined the imperfect fullerenes, which conserve the main axis of symmetry, as having topological symmetry.

* Corresponding author: Alexander I. Melker, e-mail: ndtcs@inbox.ru

3. ISOMERS OF FULLERENE C_{40}

A. ORDINARY SYMMETRY

According to the periodic system of fullerenes [1,2] there are three perfect basic fullerenes C_{40} of different ordinary symmetry, namely, four-fold, five-fold and tetrahedral one. All of them can be obtained by the mechanism known as “the fusion of fullerenes or fullerene cupolas having compatible symmetry” [3].

3.1. Fullerene C_{40} of four-fold symmetry

The fullerene was designed by the fusion of two cupolas C_{16} and C_{24} in Ref [5]; the energy was calculated in Refs. [5,6]. The fullerene is shown in Fig. 1. It consists of two tetragons, eight in-pairs adjacent pentagons and twelve hexagons forming four chains of three adjacent ones. It is a tetra₂-penta₈-hexa₁₂ polyhedron. Here the atoms are painted grey-blue; the atoms showing the main symmetry are green; the interatomic bonds are blue. In the graphs, the tetragons are painted grey, the pentagons are goldish, and the hexagons are colored yellow.

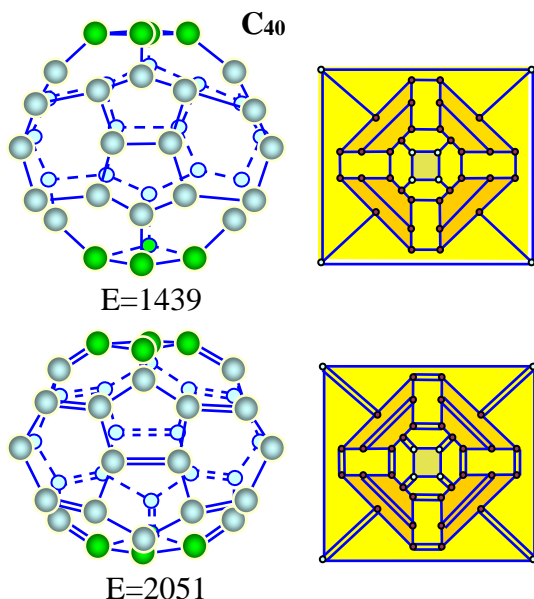


Fig. 1. Fullerene C_{40} produced by the fusion of two cupolas C_{16} and C_{24} of four-fold symmetry: structure, graphs and energy in kJ/mol.

3.2. Fullerene C_{40} of five-fold symmetry

There are two ways of joining cupolas C_{20} : mirror symmetry and rotation reflection one. The both structures were designed in Ref. [7]; the energy was calculated in Ref. [6]. In the first case the fullerene consists of five tetragons, two pentagons and fifteen hexagons and has twenty-two faces (Fig. 2). It is a tetra₅-penta₂-hexa₁₅ polyhedron. In the second case one cupola is a rotary reflection of the other

(Fig. 3). The fullerene obtained contains twelve pentagons and ten hexagons, the number of faces being the same. It is a penta₁₂-hexa₁₀ polyhedron.

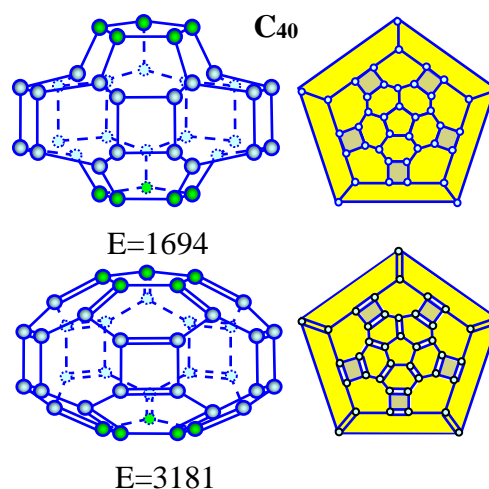


Fig. 2. Fullerene C_{40} obtained by the mirror symmetry fusion of two cupolas C_{20} of five-fold symmetry: structure, graphs and energy in kJ/mol.

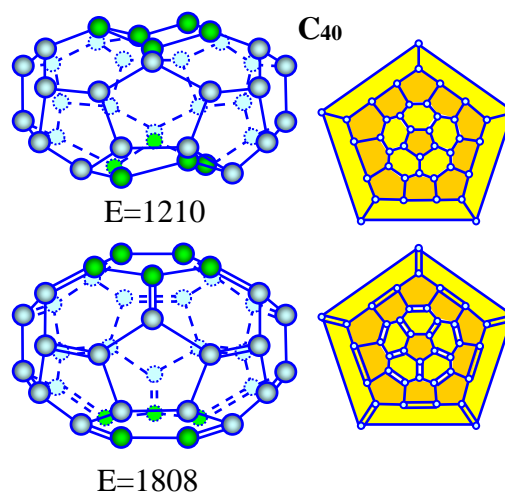


Fig. 3. Fullerene C_{40} obtained by the rotation-reflection symmetry fusion of two cupolas C_{20} of five-fold symmetry: structure, graphs and energy in kJ/mol.

3.3 Fullerene C_{40} of tetrahedral symmetry

Strictly speaking, the isomers of fullerene C_{40} were studied rather thoroughly in Ref. [7]. However, at that moment, the column of tetrahedral symmetry was not incorporated into the periodic system, we knew nothing about the existence of fullerene C_{40} having such symmetry, so it has been left beyond the scope of consideration. This drawback was corrected by the author of Ref. [8], who presented the structure of that perfect fullerene. Nevertheless, for completeness sake, it is necessary to know not only the structure, but the ways of obtaining it and its energy.

Previously, studying the formation of electronic isomers of tetrahedral fullerene C_{28} , we designed them through the use of fusion reactions [9], in particular, $C_{22}+C_6 \rightarrow (C_{22}C_6) \rightarrow C_{28}$ (fusion of a cupola with a ring) and $C_{10}+C_{18} \rightarrow (C_{10}C_{18}) \rightarrow C_{28}$ (fusion of a cupola with a bowl). It should be emphasized that in both cases the first reacting component has three-fold symmetry whereas the second refers to six-fold one. By analogy with fullerene C_{28} , it seems reasonable to investigate reaction $C_{22}+C_{18} \rightarrow (C_{22}C_{18}) \rightarrow C_{40}$, cupola C_{22} having three-fold symmetry and bowl C_{18} being of six-fold one.

The reaction is shown in Fig. 4. Here the inactive atoms are painted grey-blue; the reactive atoms are done red-green; the interatomic bonds of cupolas are blue; the new bonds between the cupolas are green. For the final fullerene C_{40} , the atoms showing three- and six-fold symmetry are specially marked, they being colored grey-turquoise. In the graph below, the pentagons are painted biscuit, the hexagons are done yellow. However, contrary to what might be expected from the addition reaction of previous cases, the fullerene obtained has no tetrahedral symmetry.

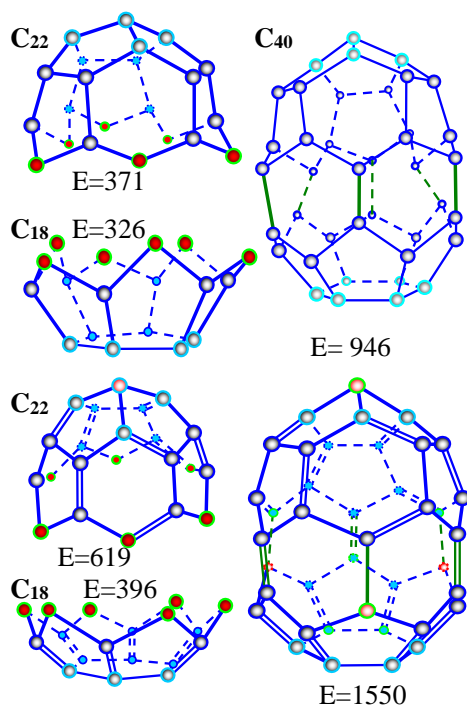


Fig. 4. Fullerene C_{40} obtained by the fusion of cupolas C_{22} with bowl C_{18} : structure, graphs and energy in kJ/mol.

Stone-Wales transformation. Sometimes an asymmetric fullerene is undergone to Stone-Wales transformation [10] that is assumed eventually may lead to the energetically most stable and symmetric isomer [11–14]. The authors [10] considered “spheroidal molecules of sp^2 hybridized carbon atoms with different arrangements of the hexagonal and pentagonal rings. A notional process for interchanging the positions of hexagons and pentagons

was illustrated. The rearrangement formally requires two sigma bonds to be broken and new bonds to be formed.” Afterwards it was more than once repeated in other studies.

However, that scheme shows only an isolated event. When one has to deal with a whole molecule where many such events take place simultaneously, to our mind, it will be more illustrative and informative to use the graph language.

For clarity’s sake, consider at first the Stone-Wales’ graph transformation for fullerene C_{40} with single bonds only (Fig. 5). Here the broken edges (bonds) are shown using red dot lines (b); the vertices (atoms) corresponding to the centers of tetrahedral symmetry are specially marked, they being painted bright-green (c); the other color designations are the same as before.

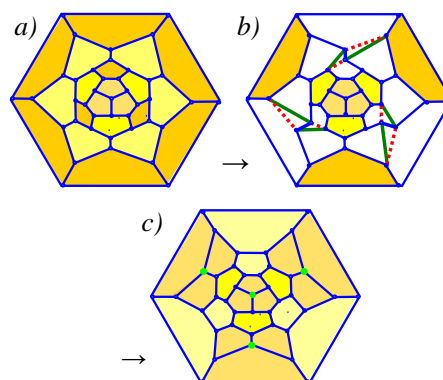


Fig. 5. Stone-Wales transformation of fullerene C_{40} obtained by fusion of cupolas C_{22} and C_{18} : a) initial three-six fold-symmetry fullerene; b) Stone-Wales transformation; c) tetrahedral fullerene.

Really, using three Stone-Wales’ transformations we obtained tetrahedral fullerene C_{40} . The problem is left: how single and double bonds are located on the fullerene surface.

The Stone-Wales’ transformation for fullerene C_{40} which takes into account the location of single and double bonds is represented in Fig. 6.

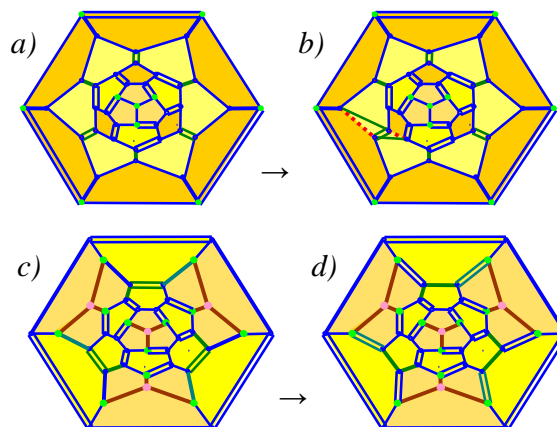


Fig. 6. Stone-Wales transformation of fullerene C_{40} with single and double bonds: a) initial three-six fold symmetry fullerene; b) Stone-Wales transformation; c) and d) tetrahedral fullerenes.

The double bonds ensure electronic symmetry and stability of the fullerene. Now all the atoms, except four atoms, are connected with other ones by one double bond and two single ones. The four atoms lying on the tetrahedral symmetry axes are painted bright-green. The edges which connect the vertices, corresponding to the centers of tetrahedral symmetry, with their neighbors are specially colored in brown (c).

The polyhedron produced is presented in Fig. 7. It contains four groups of three adjacent pentagons, ten hexagons and has twenty-two faces; therefore, it can be named symmetric $\text{penta}_{12}\text{-hexa}_{10}$ tetrahedral polyhedron C_{40} .

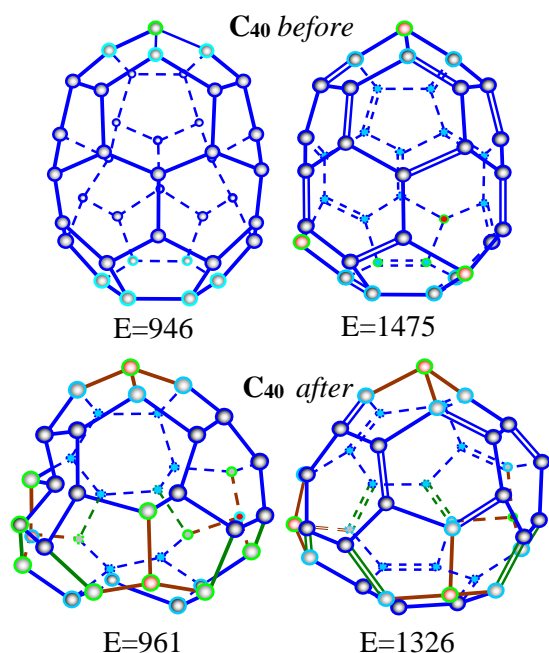


Fig. 7. Two electronic isomers of fullerene C_{40} obtained by fusion of cupola C_{22} and bowl C_{18} with the subsequent Stone-Wales transformation: structure, graphs and energy in kJ/mol.

These results deserve detailed consideration. It is known that a sphere-shaped cluster C_{60} forms at high temperature, so its structure is far removed from the structure of ideal Buckminster fullerene having I_h icosahedral symmetry. It is assumed [11] that annealing removes defects and reduces the potential energy of the cluster through the use of the Stone-Wales transformation. In our case there are no defects in the initial fullerene C_{40} having C_3 -symmetry (3-6-fold symmetry). Here the Stone-Wales transformation induces only symmetry transition from C_3 to T-symmetry (tetrahedral symmetry). This leads to decreasing the energy for the fullerene with single and double bonds that corresponds to the ground state. Yet for the fullerene with only single bonds the effect is reverse. Following the idea [14] one may assume that here the “ground” T-state is less stable and the “transition” C_3 -state is more stable. However, this is not explanation, but an ascertained fact.

B. TOPOLOGICAL SYMMETRY

According to the periodic system of fullerenes there can be three isomers C_{40} of topological symmetry [1]. They have three-fold S-symmetry, three-fold T-symmetry and six-fold one. All of them can be produced by one and the same mechanism, namely, by dimer embedding into the nearest-neighbor perfect fullerene which refers to the same column [3].

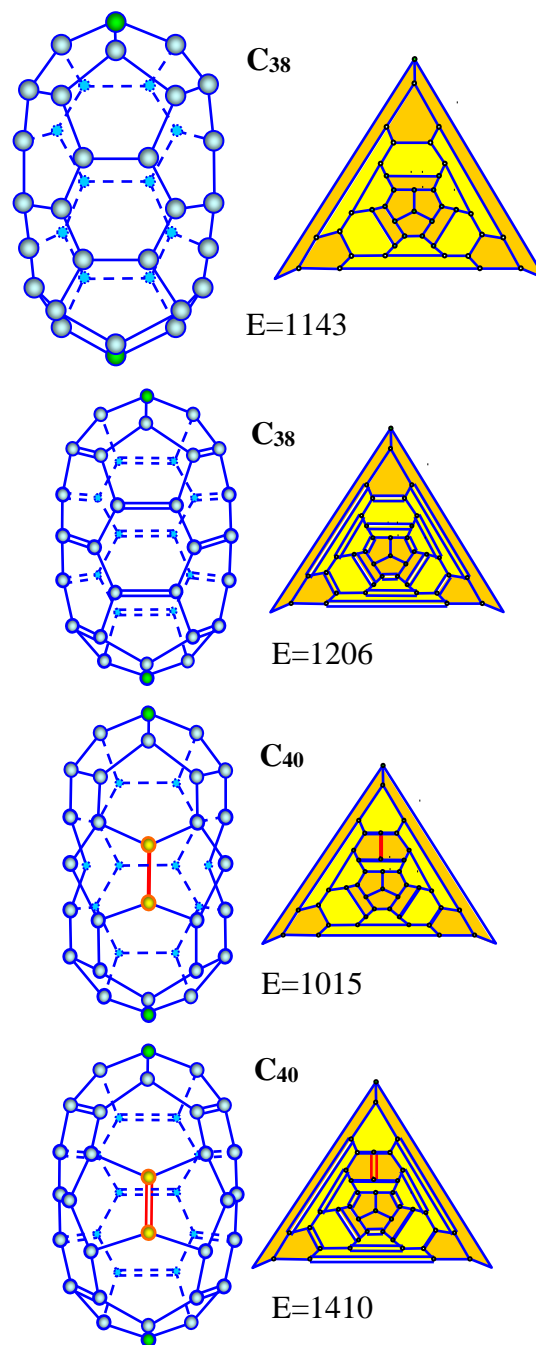


Fig. 8. Basic perfect fullerene C_{38} and its descendant, imperfect fullerene C_{40} : structure, graphs and energy in kJ/mol.

3.4. Fullerene C_{40} of three-fold S-symmetry

For fullerene C_{40} , the nearest-neighbor perfect fullerene is C_{38} , so fullerene C_{40} must contain one extra dimer. The parental fullerene and its direct descendant are designed in Ref. [15] and shown in Fig. 8. The parental fullerene contains twelve pentagons and nine hexagons; it is a $\text{penta}_{12}\text{-hexa}_9$ polyhedron. The descendant has the same number of pentagons but ten hexagons; it is a $\text{penta}_{12}\text{-hexa}_{10}$ polyhedron.

3.5. No fullerene C_{40} of three-fold T-symmetry

The nearest perfect neighbor to fullerene C_{40} is fullerene C_{36} so fullerene C_{40} could contain two extra dimers. However, fullerene C_{36} is a dead-end one. It can grow only as a nonclassical fullerene what follows from its structure shown in Fig. 9.

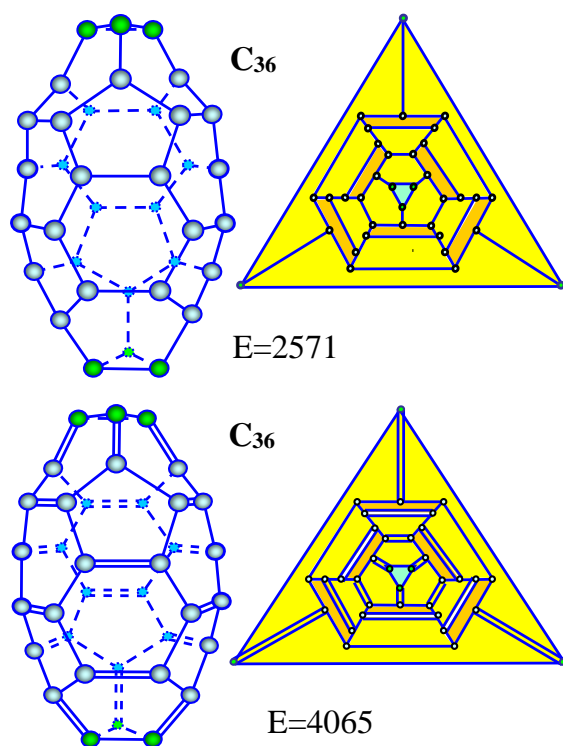


Fig. 9. Basic perfect fullerene C_{36} : structure, graphs and energy in kJ/mol.

Consider the reasons in greater detail. In principle, any fullerene can be thought over as a primary fullerene having the possibility to use for growing the mechanism known as “embedding carbon dimers.” It was suggested in 1992 by M. Endo and the future Nobel Prize winner in chemistry (1996) H.W. Kroto [16]. According to it, a carbon dimer embeds into a hexagon of an initial fullerene. This leads to stretching and breaking of the covalent bonds which are normal to the dimer and to creating new

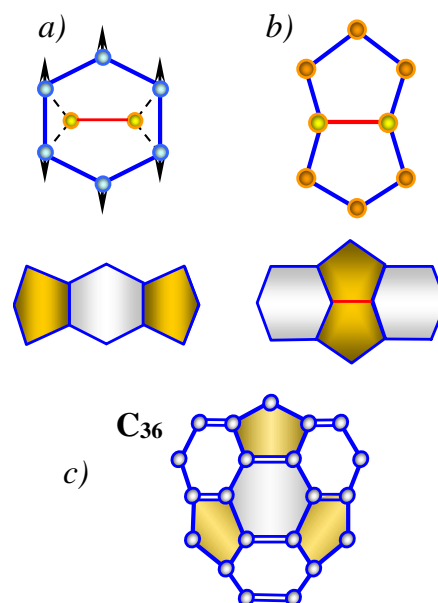


Fig. 10. a) Dimer embedding into a hexagon; b) transforming into two adjacent pentagons, c) nearest circumference of a hexagon.

bonds with the dimer (Fig. 10). As a result, there arises a new atomic configuration and there is mass increase of two carbon atoms.

However, it is necessary to take into account the nearest circumference of a hexagon (Fig. 10c).

From the figures above, of special note are the graphs, it follows that any hexagon of fullerene C_{36} has no diametrically opposite pentagons, so the fullerene is the dead-end one. That is why, we exclude fullerene C_{36} from further consideration.

3.6. Fullerene C_{40} of six-fold symmetry

The nearest perfect neighbor to fullerene C_{40} is fullerene C_{36} , so fullerene C_{40} must have two extra dimers. The parental fullerene C_{36} contains twelve pentagons and eight hexagons; it is a $\text{penta}_{12}\text{-hexa}_8$ polyhedron. The electronic isomers of parental fullerene are presented in Fig. 11. It should be emphasized that the electronic isomers with equal number but different location of single and double bonds have one and the same energy.

The descendant fullerene C_{40} consists of twelve pentagons and ten hexagons (Fig. 12). It is a $\text{penta}_{12}\text{-hexa}_{10}$ polyhedron and has three permutational isomers.

These results deserve further comment. From the Fig. 12 it follows that there are three isomers of fullerene C_{40} having one and the same topological symmetry but different shape. It is necessary to stress that we are dealing with the isomers which can be produced during the natural growth in the framework of the Endo-Kroto C_2 insertion mechanism [16].

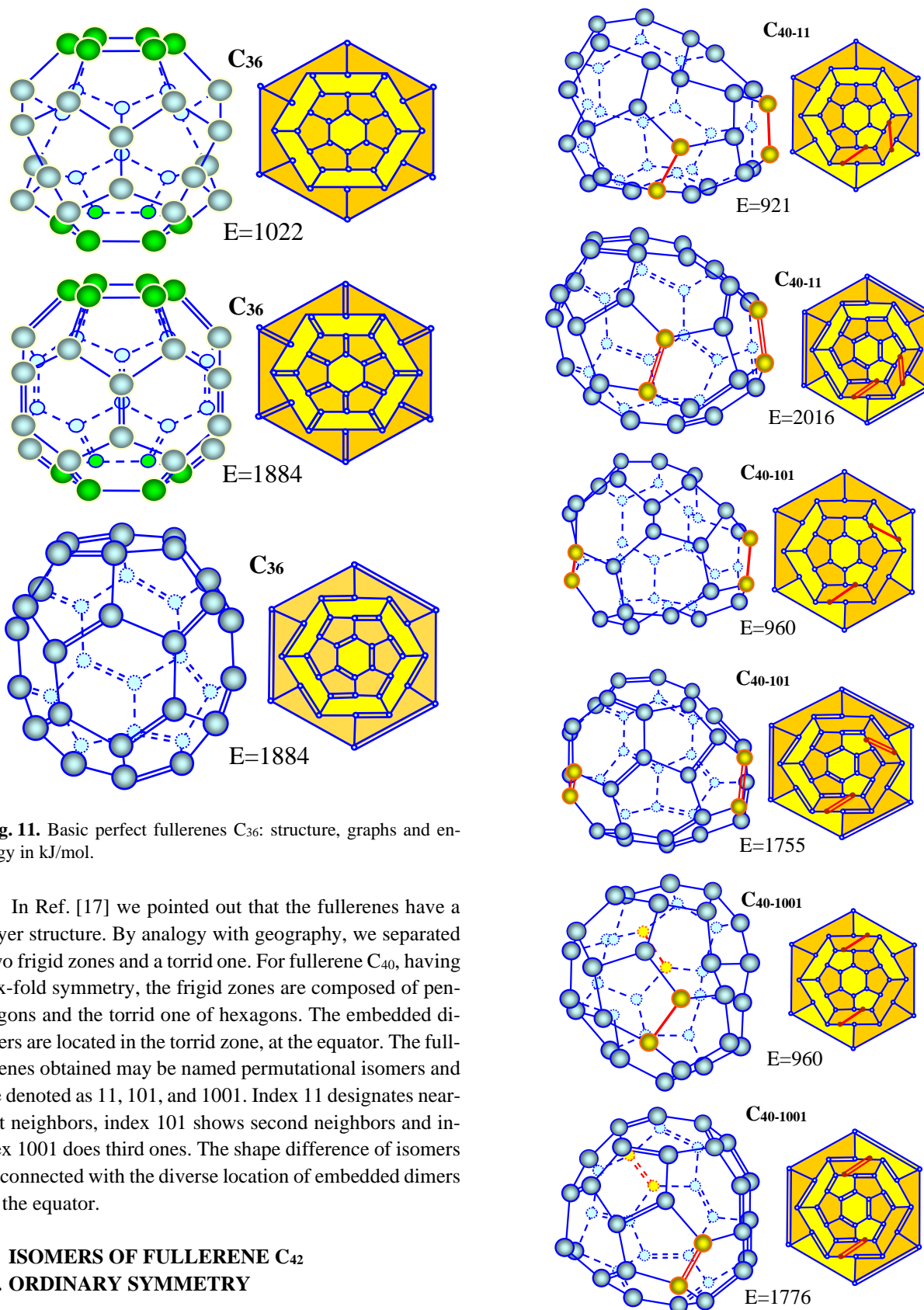


Fig. 11. Basic perfect fullerenes C₃₆: structure, graphs and energy in kJ/mol.

In Ref. [17] we pointed out that the fullerenes have a layer structure. By analogy with geography, we separated two frigid zones and a torrid one. For fullerene C₄₀, having six-fold symmetry, the frigid zones are composed of pentagons and the torrid one of hexagons. The embedded dimers are located in the torrid zone, at the equator. The fullerenes obtained may be named permutational isomers and be denoted as 11, 101, and 1001. Index 11 designates nearest neighbors, index 101 shows second neighbors and index 1001 does third ones. The shape difference of isomers is connected with the diverse location of embedded dimers at the equator.

4. ISOMERS OF FULLERENE C₄₂

A. ORDINARY SYMMETRY

According to the periodic system of fullerenes [1,2] there is only one isomer C₄₂ having ordinary three-fold T-symmetry [1].

Fig. 12. Imperfect fullerenes C₄₀: structure, graphs and energy in kJ/mol.

4.1. Fullerene C_{42} of three-fold T-symmetry

The fullerene was designed by the fusion of two cupolas C_{18} and C_{24} . It is a tri₂-penta₆-hexa₁₅ polyhedron (Fig. 13).

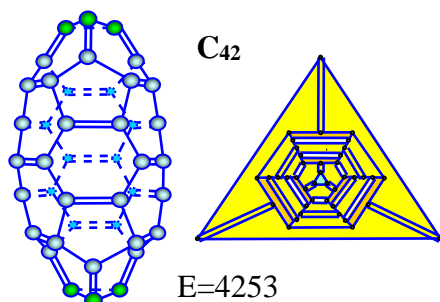


Fig. 13. Mirror symmetry fusion of two cupolas C_{18} and C_{24} of three-fold T-symmetry: structure, graphs and energy in kJ/mol.

B. TOPOLOGICAL SYMMETRY

There are five isomers C_{42} of topological symmetry [1], namely, three-fold S-symmetry, four, five- six-fold and tetrahedral ones. All of them can be obtained by one and the same mechanism, namely, by dimer embedding into the preceding nearest-neighbor fullerene of the same column; a perfect or an imperfect fullerene, it makes no difference.

4.2. Fullerene C_{42} of three-fold S-symmetry

The nearest perfect neighbor is fullerene C_{38} , so fullerene C_{42} contains two extra dimers. It consists of twelve pentagons and eleven hexagons forming a penta₁₂-hexa₁₁ polyhedron (Fig. 14).

4.3. Fullerene C_{42} of four-fold symmetry

The perfect nearest-neighbor is fullerene C_{40} , so fullerene C_{42} contains one extra dimer. It consists of two tetragons, eight pentagons and thirteen hexagons (Fig. 15). The fullerene was designed in Ref. [18]. It is a tetra₂-penta₈-hexa₁₃ polyhedron.

4.4. Fullerene C_{42} of five-fold symmetry

The perfect nearest-neighbor is fullerene C_{40} , so fullerene C_{42} contains one extra dimer. It consists of three tetragons, six pentagons and fourteen hexagons (Fig. 16). It is a tetra₃-penta₆-hexa₁₄ polyhedron.

4.5. Fullerene C_{42} of six-fold symmetry

The perfect nearest-neighbor to fullerene C_{42} is fullerene C_{36} , so fullerene C_{42} contains three extra dimers. It

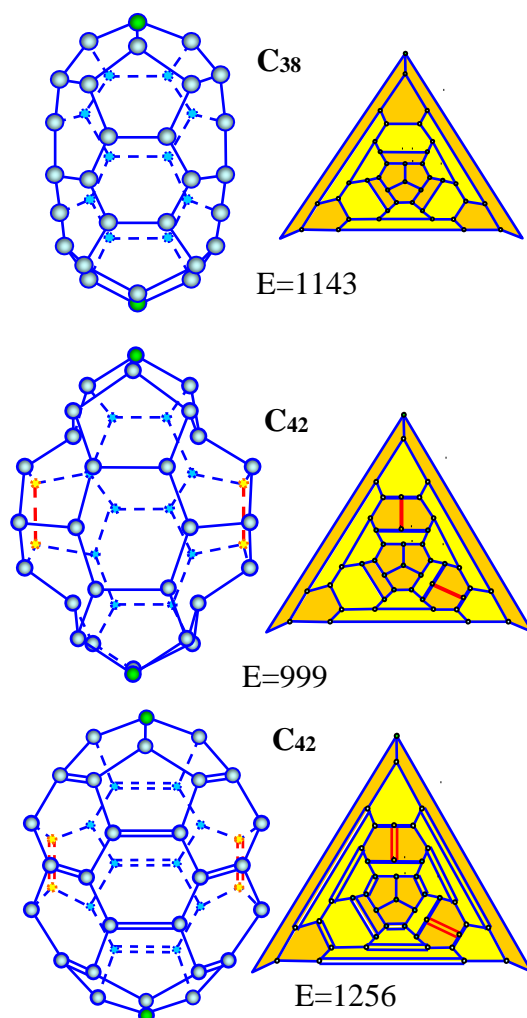


Fig. 14. Two dimers embedding into perfect fullerene C_{38} having three-fold S-symmetry: structure, graphs and energy in kJ/mol.

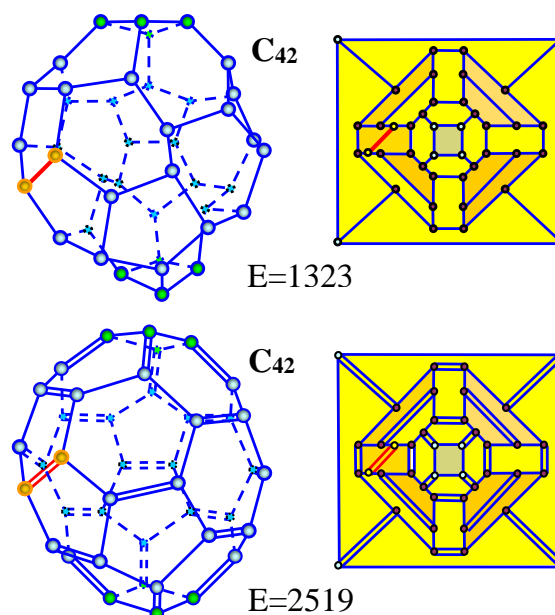


Fig. 15. Dimer embedding into perfect fullerene C_{40} having four-fold symmetry: structure, graphs and energy in kJ/mol.

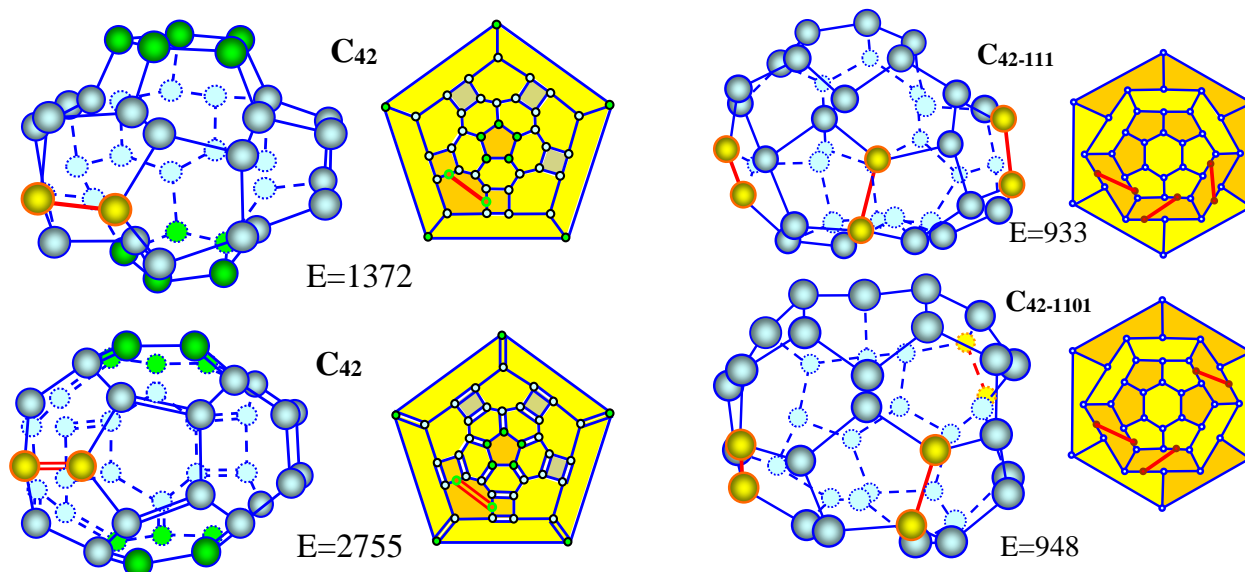


Fig. 16. Dimer embedding into perfect fullerene C_{40} having five-fold symmetry: structure, graphs and energy in kJ/mol.

consists of twelve pentagons and eleven hexagons and forms a penta₁₂-hexa₁₁ polyhedron (Fig. 17).

From the Fig. 17 follows that there are three isomers of fullerene C_{42} having one and the same topological symmetry but different shape. As in the case of the isomers of fullerene C_{40} having six-fold topological symmetry, the shape difference is connected with the diverse location of embedded dimers in the torrid zone, at the equator. The fullerenes obtained will be named permutation isomers and be denoted as 111, 1101 and 10101. Index 111 indicates that between the embedded dimers there are no hexagon sites; index 1101 points to the fact that two dimers are the nearest neighbors, and index 10101 designates that all the three dimers are second neighbors.

4.6. Fullerene of tetrahedral symmetry

The nearest perfect neighbor is fullerene C_{40} , so fullerene C_{42} contains one extra dimer. It consists of two groups of three adjacent pentagons, a chain of six pentagons and eleven hexagons, and has twenty-three faces. Therefore, it can be named imperfect penta₁₂-hexa₁₁ polyhedron C_{42} having topological tetrahedral symmetry (Fig. 18).

5. ISOMERS OF FULLERENE C_{44}

A. ORDINARY SYMMETRY

According to the periodic system of fullerenes [1] there is only one isomer C_{44} having ordinary three-fold S -symmetry [1].

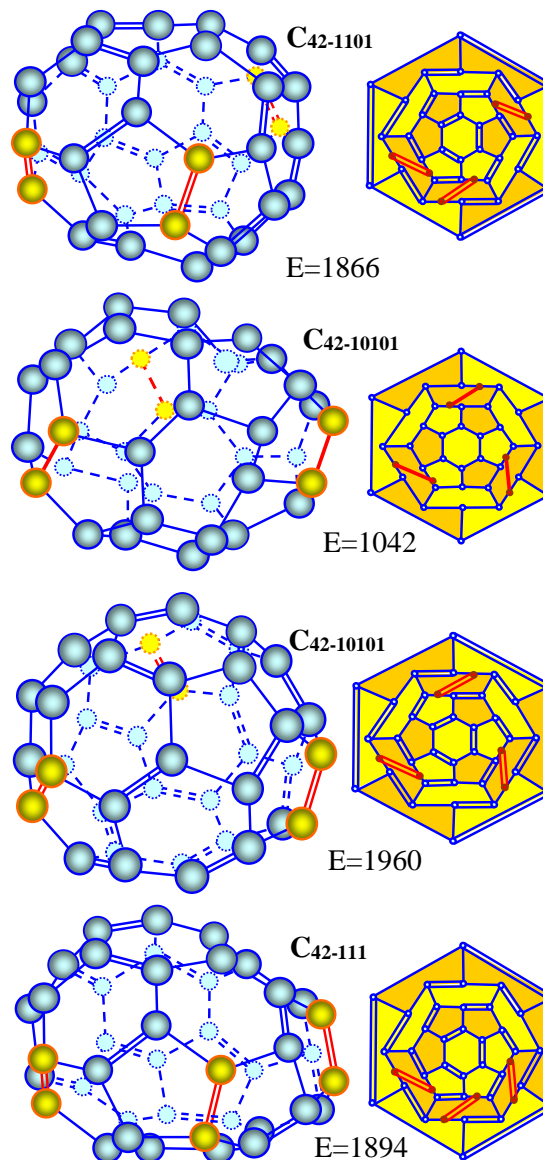


Fig. 17. Three dimers embedding into perfect fullerene C_{36} having six-fold symmetry: structure, graphs and energy in kJ/mol.

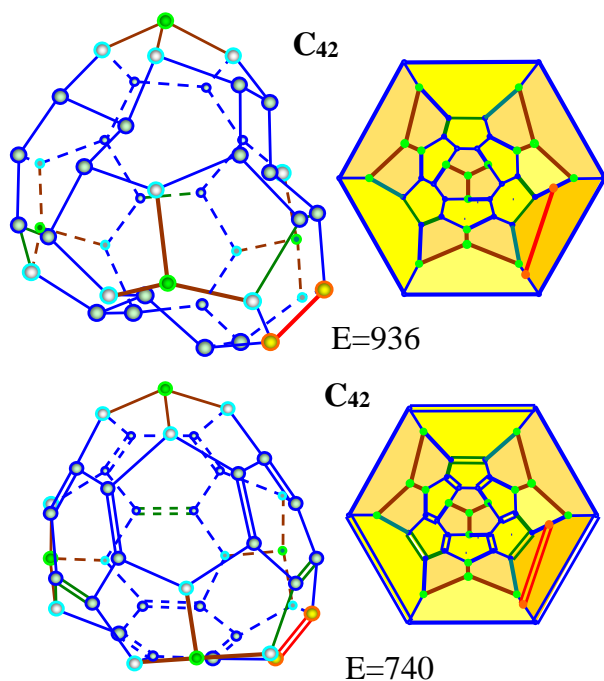


Fig. 18. Dimer embedding into perfect fullerene C_{40} having tetrahedral symmetry: structure, graphs and energy in kJ/mol.

5.1. Fullerene of three-fold S-symmetry

It can be produced by the mechanism known as the fusion of fullerenes or fullerene cupolas having compatible symmetry [3]. The fullerene was designed by the fusion of two cupolas C_{22} in Ref. [15] and is shown in Fig. 19. It contains two groups of six adjacent pentagons at the top and bottom, and twelve hexagons. It is a (penta-hexa)₁₂ polyhedron.

B. TOPOLOGICAL SYMMETRY

According to the periodic system of fullerenes there are five isomers C_{44} having topological symmetry [1], namely, three-fold T-symmetry, four-, five-, six-fold and tetrahedral ones. All of them can be obtained by dimer embedding into the perfect nearest-neighbor fullerene which precedes it in the same column.

5.2. Fullerene of three-fold T-symmetry

The perfect nearest neighbor is fullerene C_{42} , so fullerene C_{44} must contain one extra dimer. It consists of two trigons, four isolated pentagons, two adjacent pentagons, sixteen hexagons and has twenty-four faces. It is a tri₂-penta₆-hexa₁₆ polyhedron (Fig. 20).

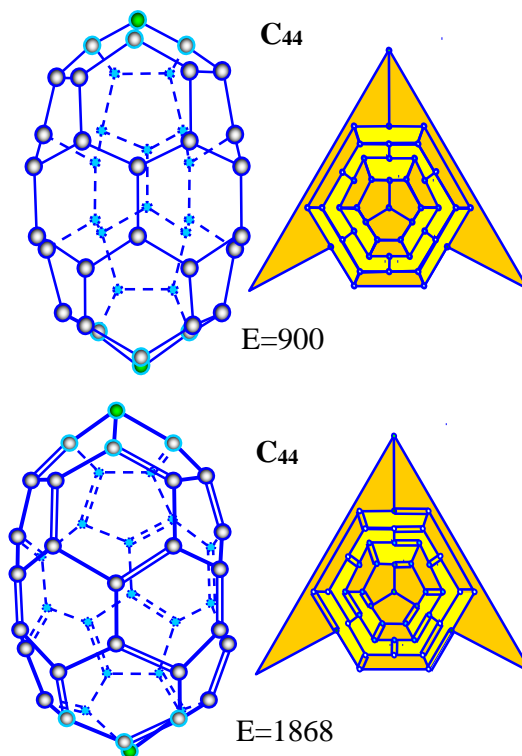


Fig. 19. Basic perfect fullerenes C_{44} : structure, graphs and energy in kJ/mol.

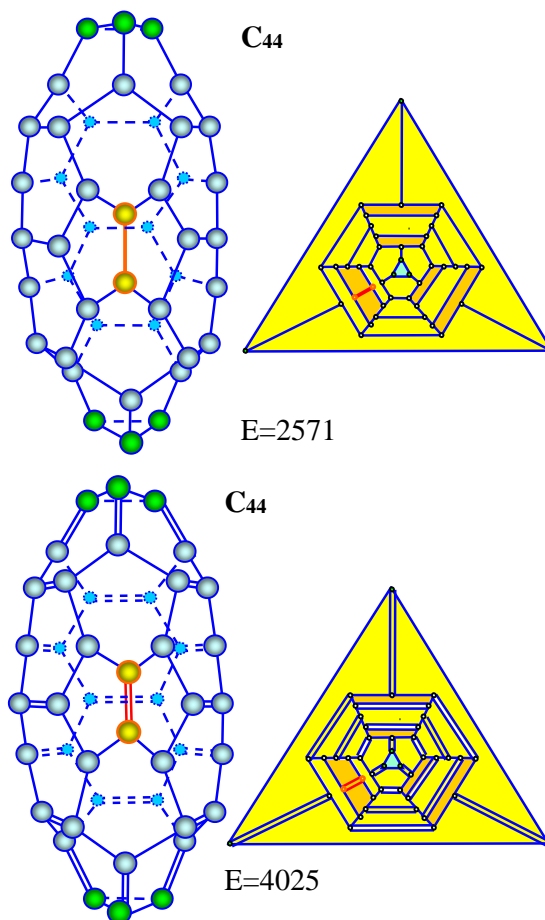


Fig. 20. Dimer embedding into perfect fullerene C_{42} of three-fold T-symmetry: structure, graphs and energy in kJ/mol.

5.3. Fullerene C_{44} of four-fold symmetry

The perfect nearest-neighbor is fullerene C_{40} , so fullerene C_{44} contains two extra dimers. The fullerene was designed in Ref. [18]. It consists of two tetragons, eight pentagons and fourteen hexagons. It is a tetra₂-penta₈-hexa₁₄ polyhedron (Fig. 21).

From the figure follows that there are two isomers of fullerene C_{44} having one and the same topological four-fold symmetry but different shape. Similar to the isomers

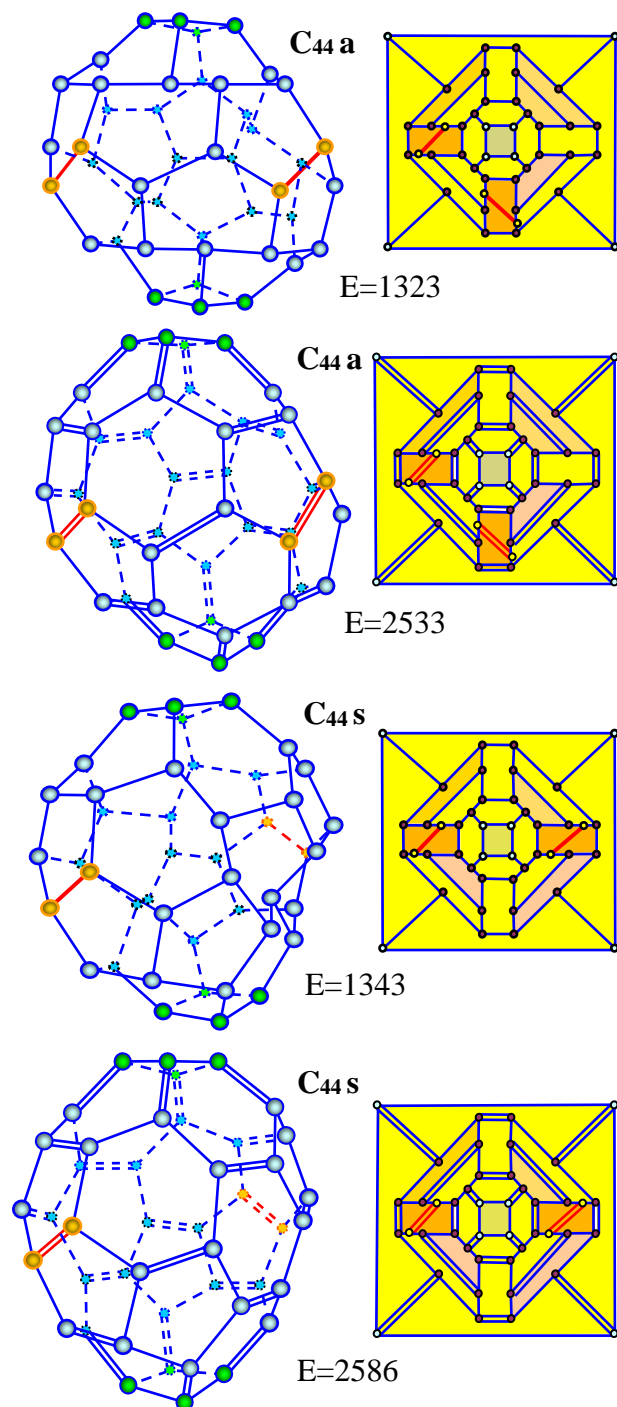


Fig. 21. Two dimers embedding into perfect fullerene C_{40} having four-fold symmetry: structure, graphs and energy in kJ/mol.

of fullerene C_{42} of topological six-fold symmetry, the shape difference is induced by the diverse location of embedded dimers. The fullerenes obtained are permutation isomers and be denoted as **a** and **s**. Index **a** indicates that the embedded dimers are located in one and the same hemisphere, i.e., asymmetrically with respect to the main axis of symmetry; index **s** points to the fact that the dimers refer to different hemispheres and are located symmetrically.

5.4. Fullerene C_{44} of five-fold symmetry

The perfect nearest-neighbor is fullerene C_{40} , so fullerene C_{44} must contain two extra dimers. It consists of two tetragons, six pentagons and fourteen hexagons (Fig. 22). It is a tetra₂-penta₆-hexa₁₄ polyhedron.

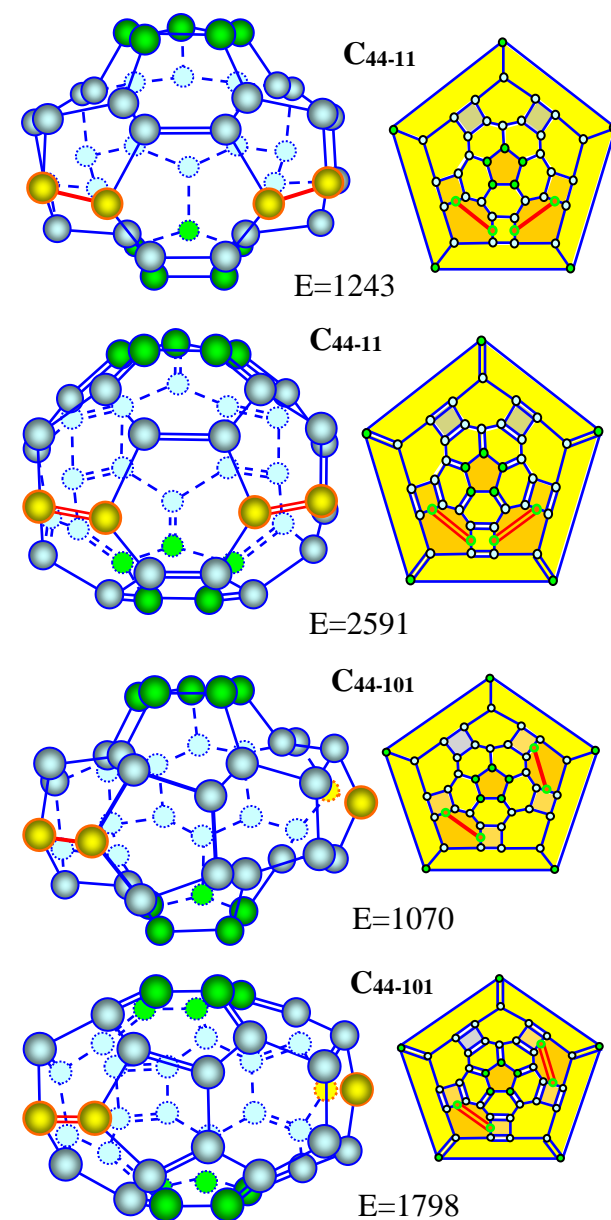


Fig. 22. Two dimers embedding into perfect fullerene C_{40} having five-fold symmetry: structure, graphs and energy in kJ/mol.

One can see that there are two isomers of fullerene C_{44} having one and the same topological five-fold symmetry but different shape. They are permutation isomers. The embedded dimers are located at the equator. The fullerenes obtained may be denoted as 11 and 101. Index 11 designates nearest neighbors; index 101 shows second neighbors. The shape and energy difference of isomers is connected with the diverse location of embedded dimers at the equator.

5.5. Fullerene C_{44} of six-fold symmetry

The perfect nearest-neighbor to fullerene C_{44} is fullerene C_{36} , so fullerene C_{44} contains four extra dimers. It consists of twelve pentagons and twelve hexagons (Fig. 23). It is a penta₁₂-hexa₁₂ polyhedron.

There are three isomers of fullerene C_{44} having one and the same topological symmetry but different shape. As in the case of the isomers of fullerene C_{42} having six-fold topological symmetry, the shape difference is connected with the diverse location of embedded dimers in the torrid zone, at the equator. The fullerenes obtained may be named permutation isomers and be denoted as 1111, 11101 and 11011. Index 1111 indicates that between the embedded dimers there is no hexagon sites; index 11101 points to the fact that only three dimers are the nearest neighbors, and index 11011 designates that there are two groups of two adjacent dimers.

5.6. Fullerene C_{44} of tetrahedral symmetry

The nearest perfect neighbor is fullerene C_{40} , so fullerene C_{44} contains two extra dimers. It consists of two groups of three adjacent pentagons, a chain of six pentagons and eleven hexagons, and has twenty-three faces (Fig. 24). Therefore, it can be named imperfect penta₁₂-hexa₁₁ polyhedron C_{42} having topological tetrahedral symmetry.

6. ISOMERS OF FULLERENE C_{46}

A. ORDINARY SYMMETRY

There is no isomers C_{46} having ordinary symmetry [1,2].

B. TOPOLOGICAL SYMMETRY

According to the periodic system all six fullerene isomers C_{46} refer to topological symmetry [1], namely, three-fold S-symmetry, three-fold T-symmetry, four-, five-, six-fold and tetrahedral ones. All of them can be obtained by one and the same mechanism, namely, by dimer embedding into the nearest neighbor perfect or imperfect fullerene which precedes it in the same column.

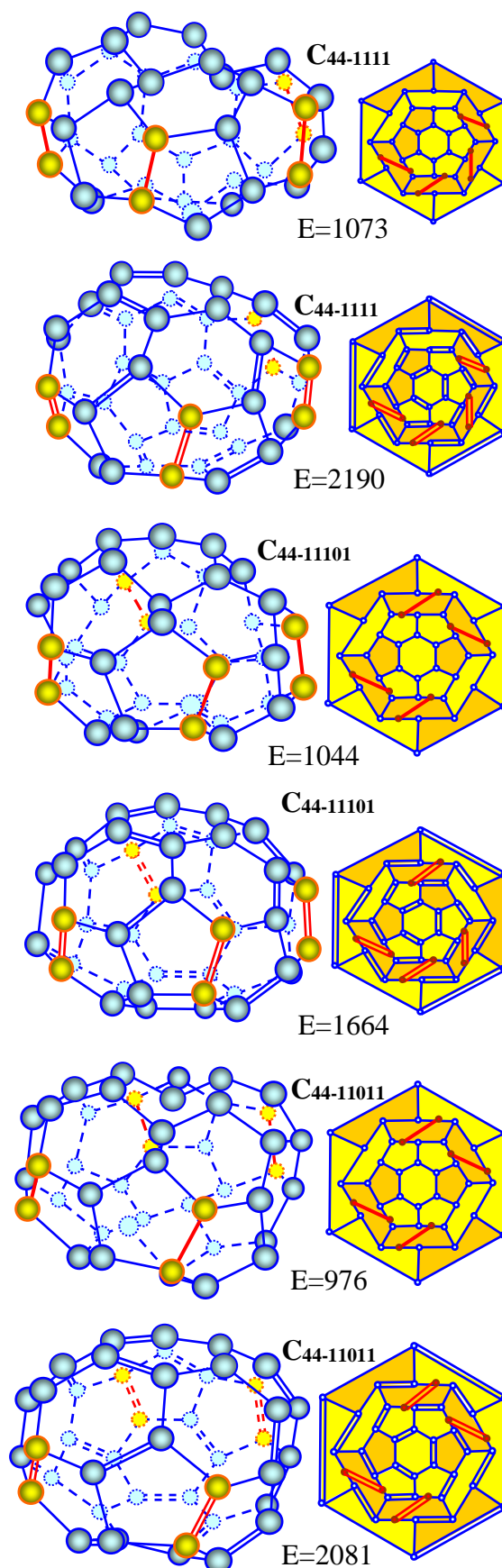


Fig. 23. Permutation isomers of fullerene C_{44} of six-fold symmetry: structure, graphs and energy in kJ/mol.

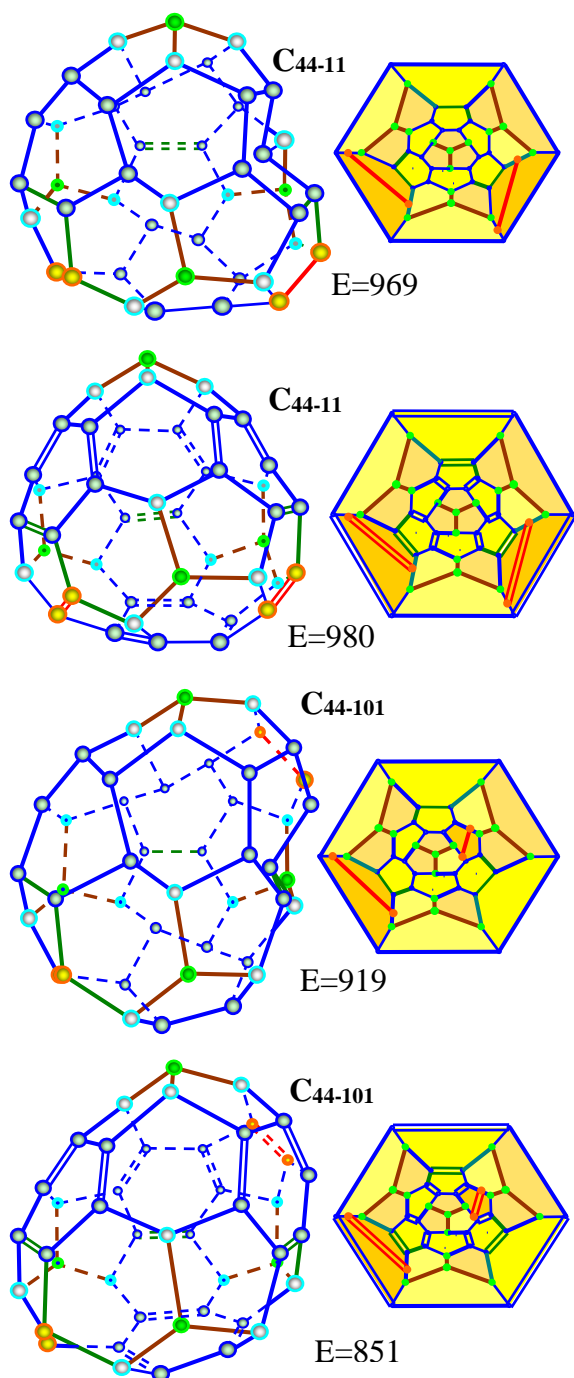


Fig. 24. Two dimers embedding into perfect fullerene C_{40} having tetrahedral symmetry: structure, graphs and energy in kJ/mol.

6.1. Fullerene of three-fold S-symmetry

The perfect nearest neighbor is fullerene C_{44} , so fullerene C_{44} must contain one extra dimer. The fullerene was designed in Ref. [15] and is shown in Fig. 25. It contains two nonequivalent groups of six adjacent pentagons at the top and bottom, and thirteen hexagons. It is a $\text{penta}_{12}\text{-hexa}_{13}$ polyhedron.

6.2. Fullerene of three-fold T-symmetry

The fullerene can be produced by embedding two dimers C_2 into the nearest perfect fullerene C_{42} . It consists of two trigons, four isolated pentagons, two adjacent pentagons, sixteen hexagons and has twenty-four faces (Fig. 26). It is a $\text{tri}_2\text{-penta}_6\text{-hexa}_{16}$ polyhedron.

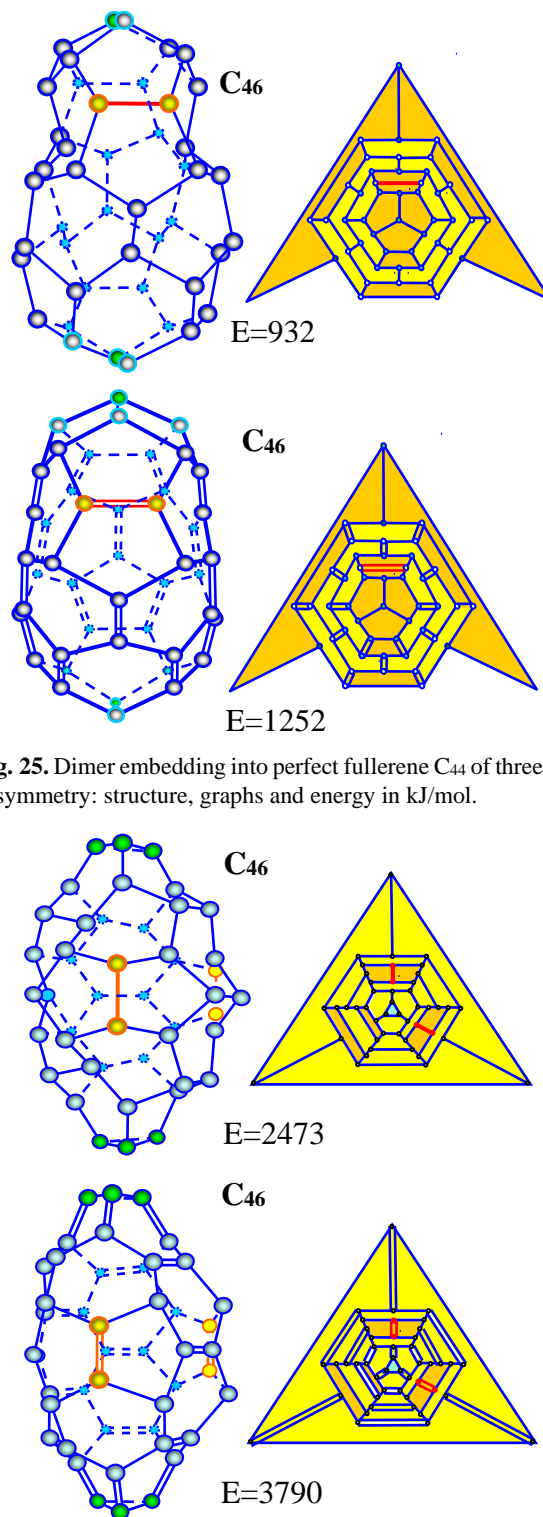


Fig. 25. Dimer embedding into perfect fullerene C_{44} of three-fold S-symmetry: structure, graphs and energy in kJ/mol.

Fig. 26. Two dimers embedding into perfect fullerene C_{42} having three-fold T-symmetry: structure, graphs and energy in kJ/mol.

6.3. Fullerene C_{46} of four-fold symmetry

The perfect nearest-neighbor is fullerene C_{40} , so fullerene C_{46} contains three extra dimers. It consists of two tetragons, eight pentagons and fourteen hexagons (Fig. 27). It is a tetra₂-penta₈-hexa₁₄ polyhedron.

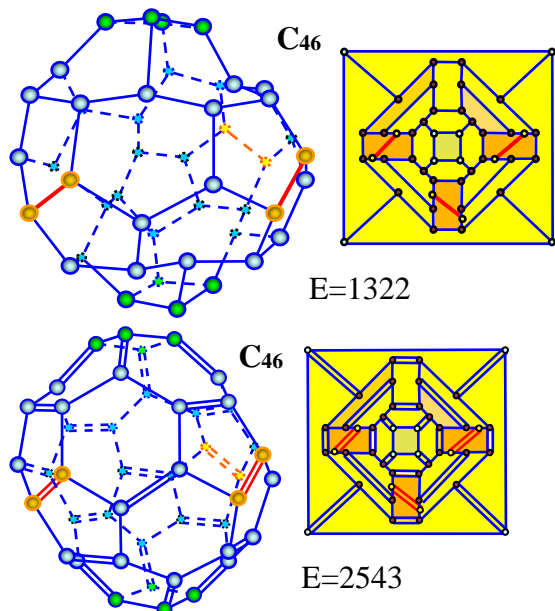


Fig. 27. Three dimers embedding into perfect fullerene C_{40} having four-fold symmetry: structure, graphs and energy in kJ/mol.

6.4. Fullerene C_{46} of five-fold symmetry

The perfect nearest-neighbor is fullerene C_{40} , so fullerene C_{44} must contain three extra dimers. It consists of two tetragons, six pentagons and fourteen hexagons (Fig. 28). It is a tetra₂-penta₈-hexa₁₄ polyhedron.

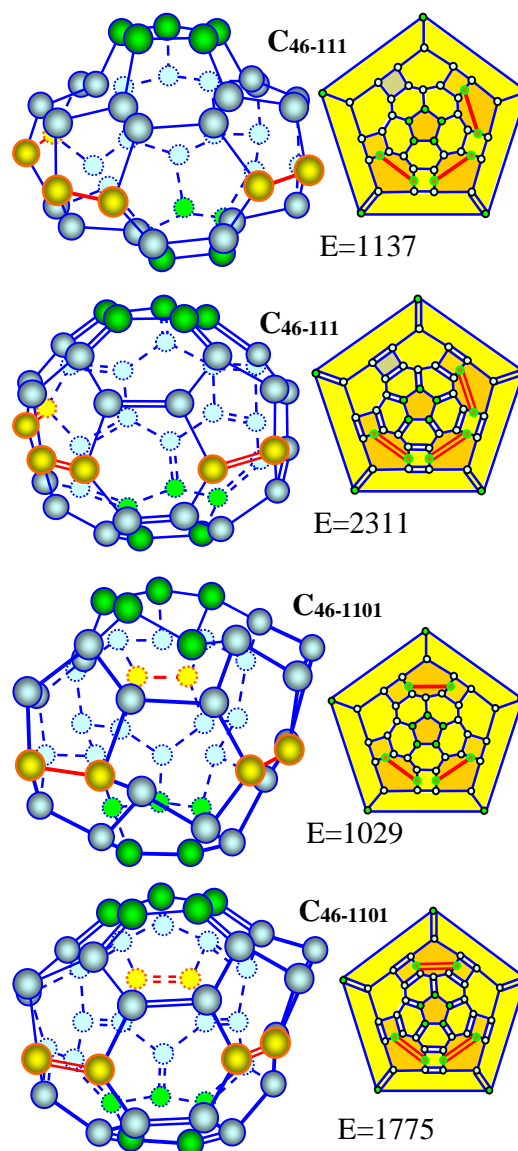


Fig. 28. Three dimers embedding into perfect fullerene C_{40} having five-fold symmetry: structure, graphs and energy in kJ/mol.

6.5. Fullerene C_{46} of six-fold symmetry

The perfect nearest-neighbor to fullerene C_{46} is fullerene C_{36} , so fullerene C_{46} contains five extra dimers. It consists of twelve pentagons and twelve hexagons (Fig. 29). It is a penta₁₂-hexa₁₂ polyhedron.

6.6. Fullerene C_{46} of tetrahedral symmetry

The nearest perfect neighbor is fullerene C_{40} , so fullerene C_{46} contains three extra dimers. It consists of two groups of three adjacent pentagons, a chain of six pentagons and eleven hexagons, and has twenty-three faces (Fig. 30). It is an imperfect penta₁₂-hexa₁₁ polyhedron having topological tetrahedral symmetry.

The fullerenes obtained may be named permutation isomers and be denoted as 111-ring, 111-cobra and 111-star. Index 111 indicates that there are three embedded dimers; the words ring, snake and star characterize their

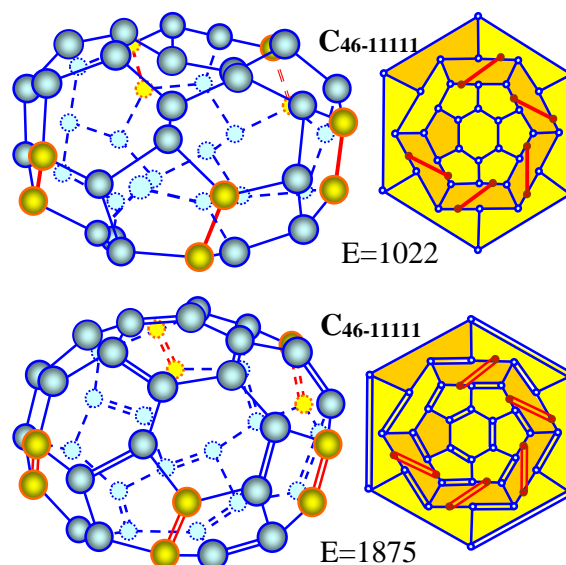


Fig. 29. Five dimers embedding into perfect fullerene C_{36} having six-fold symmetry: structure, graphs and energy in kJ/mol.

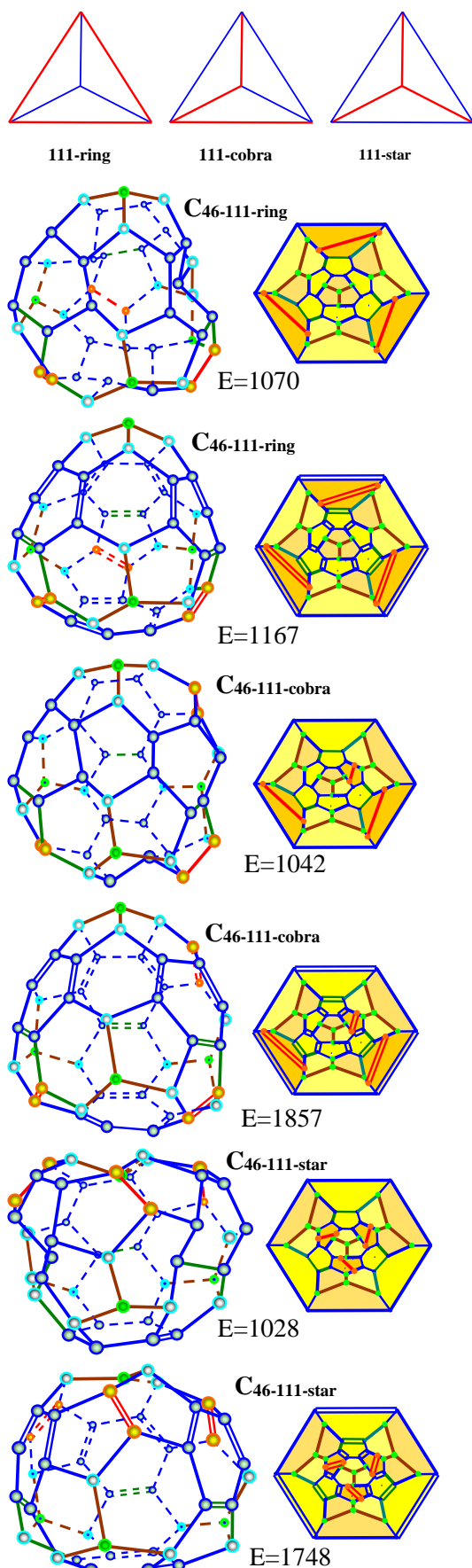


Fig. 30. Three ways of three dimers embedding into perfect fullerene C_{40} : structure, graphs and energy in kJ/mol.

position as shown below. It should be emphasized that there are only six possible sites (tetrahedral graph edges). The occupied sites are colored red.

7. ISOMERS OF FULLERENE C_{48}

A. ORDINARY SYMMETRY

There are three isomers C_{48} of ordinary different symmetry [1,2], namely, having three-fold T-symmetry, having four- and six-fold symmetry.

7.1. Fullerene of three-fold T-symmetry

One can design two fullerene isomers of this symmetry by two ways: by the fusion of two cupolas C_{24} and as a result of embedding one after another three carbon dimers into fullerene C_{42} [13]. The isomers are shown in Fig. 31. Both polyhedrons contain two triangles, six pentagons and eighteen hexagons, so they are $\text{tri}_2\text{-penta}_6\text{-hexa}_{18}$ polyhedrons. Formally they are both fullerenes. However, we admit that the first isomer is a nanotube. The reason for such conclusion is discussed elsewhere [13].

7.2. Fullerene C_{48} of four-fold symmetry

Similar to the previous case, one can design two fullerene isomers of this symmetry by two ways: by the fusion of two cupolas C_{24} and as a result of embedding one after another four carbon dimers into fullerene C_{40} [18]. The isomers are shown in Fig. 32. Both polyhedrons contain two tetragons, eight pentagons and sixteen hexagons, so they are $\text{tetra}_2\text{-penta}_8\text{-hexa}_{16}$ polyhedrons.

The shape difference is also dictated by the specific location of pentagons. The number of pentagons is the same, but the first isomer contains isolated pentagons along the main axis of symmetry, whereas the pentagons of the second one are arranged in adjacent pairs at an angle to this axis. As a result, both isomers look like a spheroid. Probably, because of this they have almost equal energy.

7.3. Fullerene C_{48} of six-fold symmetry

As before, one can design two fullerene isomers of this symmetry by two different ways: by the fusion of two cupolas C_{24} and as a result of successive embedding six carbon dimers into basic perfect fullerene C_{36} of six-fold symmetry. However, for this symmetry there are two modes of cupola joining: mirror symmetry and rotation-reflection one. In the first case the lower cupola is a mirror copy of the upper one. The fullerene obtained consists of six tetragons and twenty hexagons; it has twenty-six

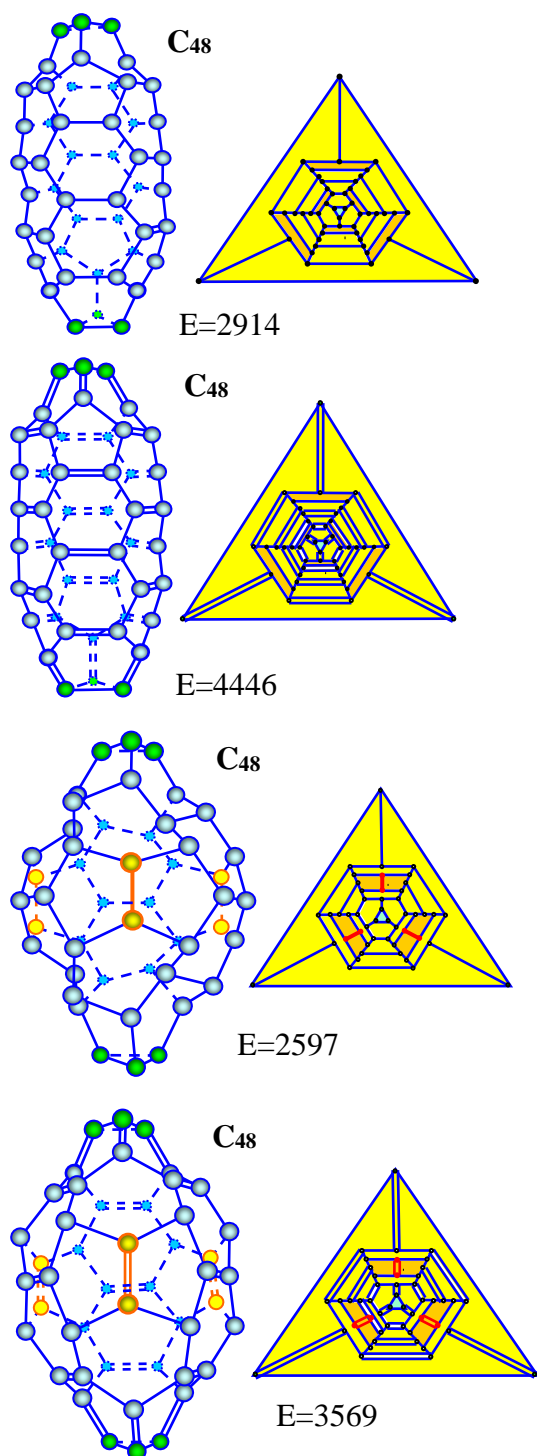


Fig. 31. Fullerene C_{48} as a result of rotation-reflection symmetry fusion of two cupolas C_{24} having three-fold symmetry and obtained by embedding one after another three carbon dimers into perfect fullerene C_{42} ; structure, graphs and energy in kJ/mol.

faces (Fig. 33). It is a $\text{tetra}_6\text{-hexa}_{20}$ polyhedron. In the second case the lower cupola is a rotatory reflection of the upper one. The fullerene obtained contains twelve pentagons and ten hexagons, the number of faces being the same (Fig. 34). It is a $\text{penta}_{12}\text{-hexa}_{14}$ polyhedron. Its energy is less than that of the first fullerene.

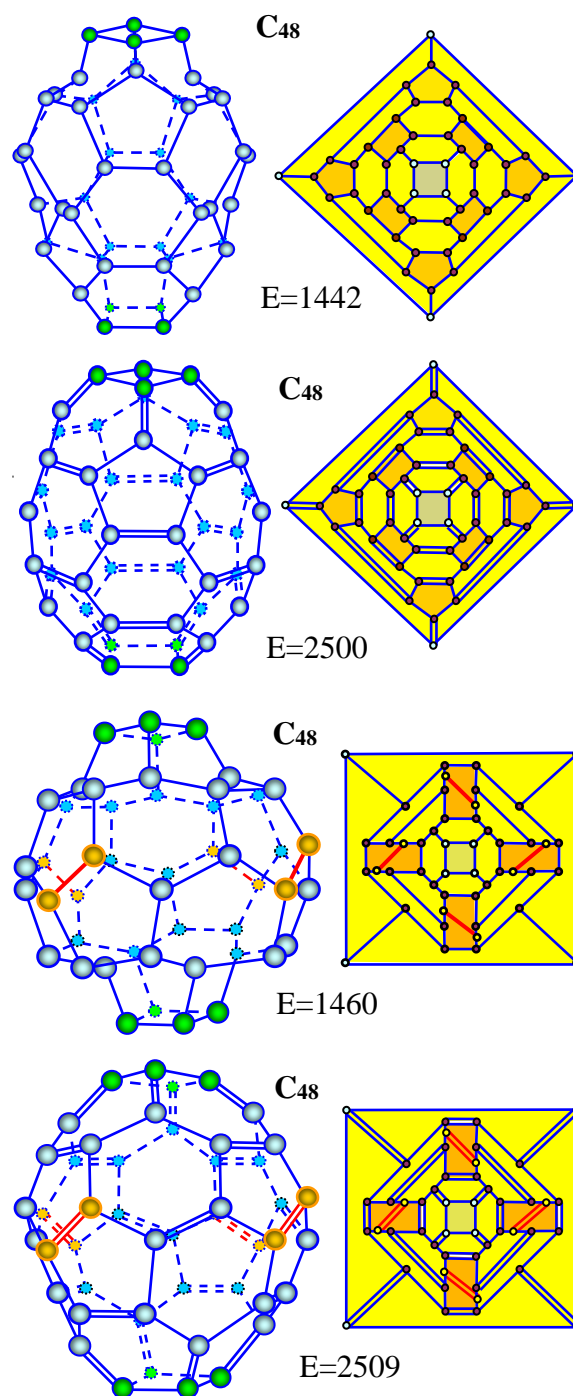


Fig. 32. Fullerene C_{48} as a result of rotation-reflection symmetry fusion of two cupolas C_{24} having four-fold symmetry (above); fullerenes C_{48} obtained by embedding one after another four carbon dimers into perfect fullerene C_{40} (below): structure, graphs and energy in kJ/mol.

Consider the second way of fullerene generation: the growth of basic perfect ancestor by successive embedding carbon dimers, the number of dimers being equal to the symmetry order. The perfect nearest-neighbor to fullerene C_{48} is fullerene C_{36} , so fullerene C_{48} contains six extra dimers. It consists of twelve pentagons and

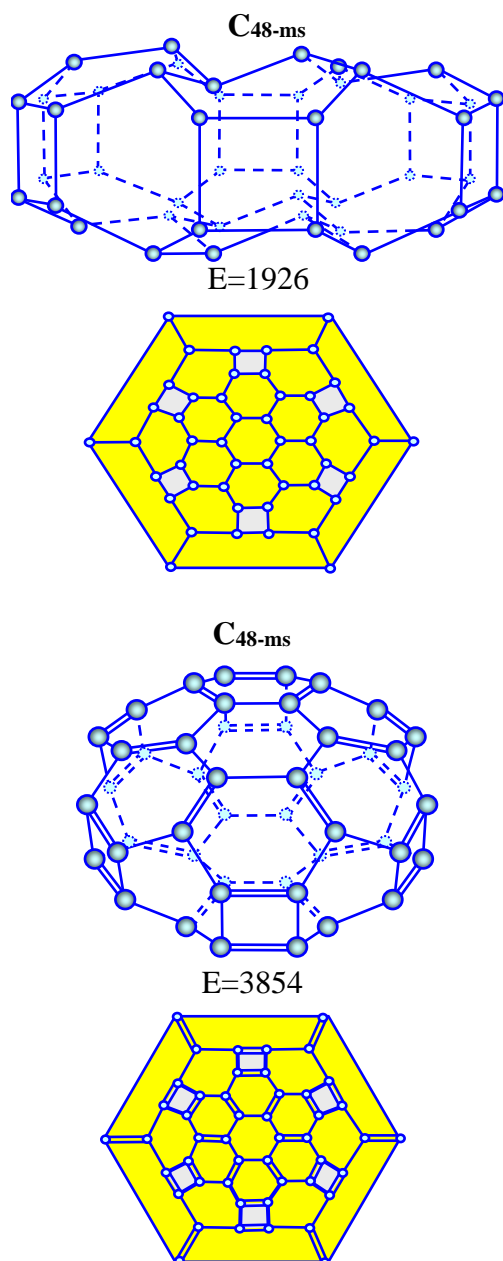


Fig. 33. Fullerene C_{48} as a result of the fusion of two cupolas C_{24} having six-fold symmetry by mirror symmetry joining: structure, graphs and energy in kJ/mol.

fourteen hexagons (Fig. 35). It is a $\text{penta}_{12}\text{-hexa}_{14}$ polyhedron.

There is also the third way of new fullerene generations: fusion of lesser fullerenes having compatible symmetry. In our case there are two fullerenes C_{24} of six-fold symmetry which can be combined for producing fullerene C_{48} (Fig. 36).

B. TOPOLOGICAL SYMMETRY

According to the periodic system of fullerenes there are three isomers C_{48} having topological symmetry [1], namely,

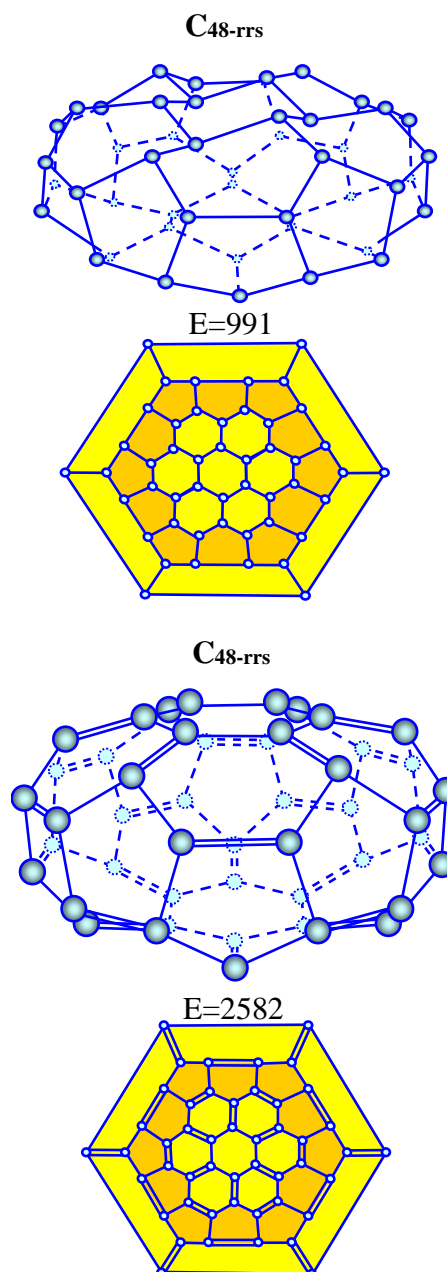


Fig. 34. Fullerene C_{48} as a result of the fusion of two cupolas C_{24} having six-fold symmetry by rotation-reflection symmetry joining: structure, graphs and energy in kJ/mol.

three-fold S -symmetry, five- and tetrahedral ones. All of them can be obtained by one and the same mechanism, namely, by dimer embedding into the nearest neighbor perfect fullerene which precedes it to in the same column.

7.4. Fullerene of three-fold S -symmetry

The perfect nearest neighbor to fullerene C_{48} is fullerene C_{44} , so C_{48} fullerene must contain two extra dimers. There are two isomers of fullerene C_{48} having one and the same topological symmetry but different location of dimers. They are shown in Fig. 37. Each one contains two nonequivalent

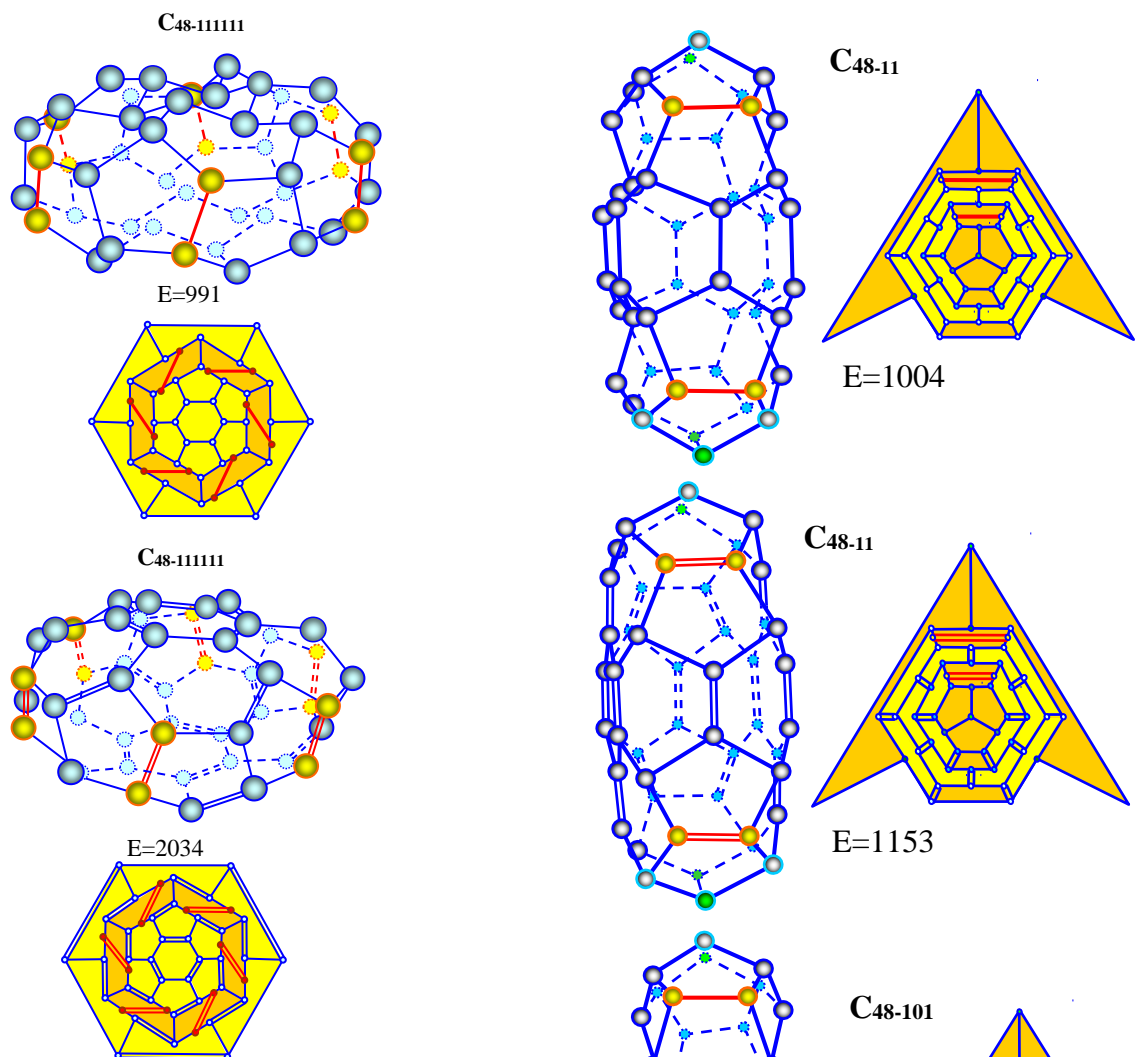


Fig. 35. Six dimers embedding into perfect fullerene C_{36} having six-fold symmetry; structure, graphs and energy in kJ/mol.

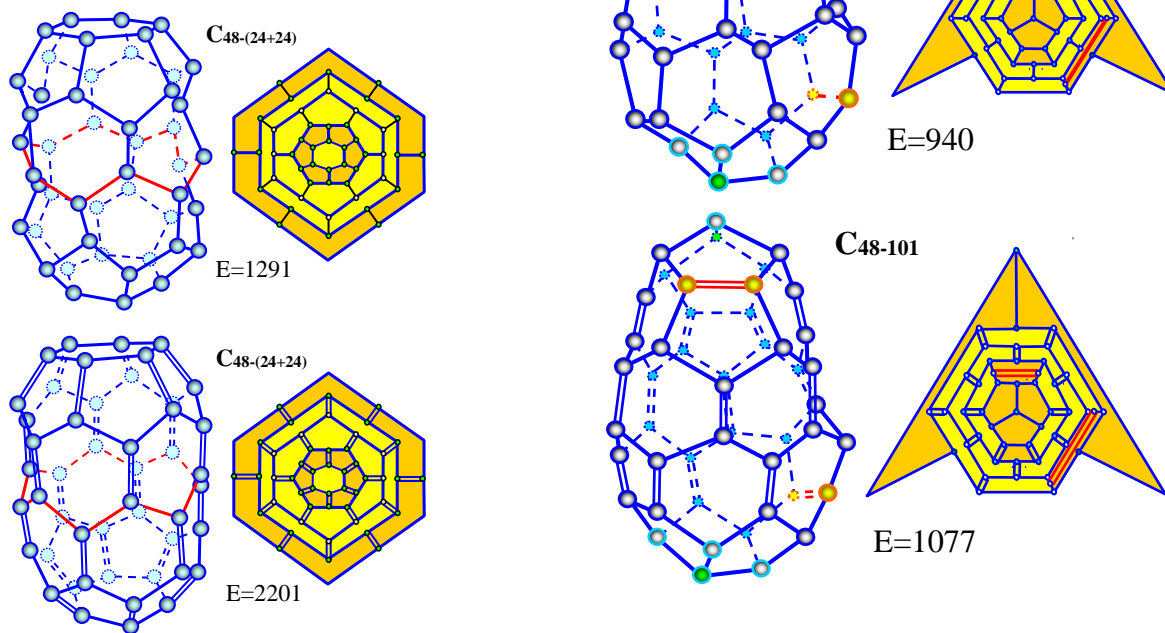


Fig. 36. Fullerene C_{48} as a result of joining two fullerenes C_{24} having six-fold symmetry; rotation-reflection symmetry joining: structure, graphs and energy in kJ/mol.

Fig. 37. Two dimers embedding into perfect fullerene C_{44} of three-fold S-symmetry, symmetric embedding and asymmetric one: structure, graphs and energy in kJ/mol.

groups of six adjacent pentagons at the top and bottom, and thirteen hexagons. However, each one is a penta₁₂-hexa₁₃ polyhedron.

The shape difference is connected with the diverse location of embedded dimers. The fullerenes obtained may be named permutation isomers and be denoted as 11 and 101. Index 11 indicates that the embedded dimers are in one and the same of three possible cylindrical sectors; index 101 points to the fact that two dimers are at different ones.

7.5. Fullerene C₄₈ of five-fold symmetry

The perfect nearest-neighbor is fullerene C₄₀, so fullerene C₄₈ must contain four extra dimers. It consists of twelve pentagons and fourteen hexagons (Fig. 38). It is a penta₁₂-hexa₁₄ polyhedron.

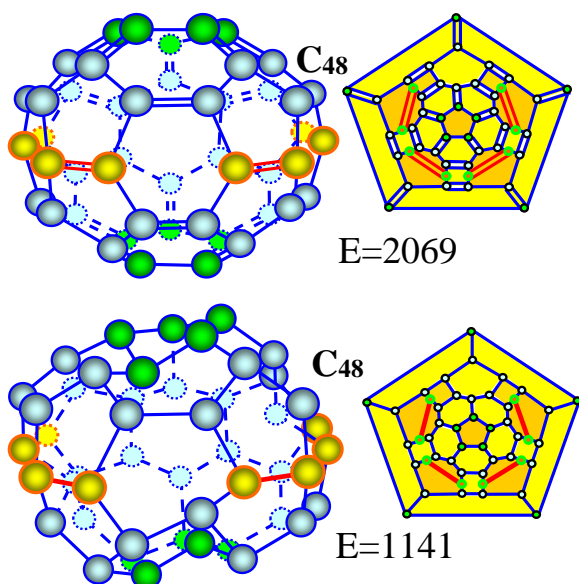


Fig. 38. Four dimers embedding into perfect fullerene C₄₀ having five-fold symmetry: structure, graphs and energy in kJ/mol.

7.6. Fullerene C₄₈ of tetrahedral symmetry

The nearest perfect neighbor is fullerene C₄₀, so fullerene C₄₈ contains four extra dimers. It consists of three or four groups of twelve adjacent pentagons and thirteen hexagons (Fig. 39). It is imperfect penta₁₂-hexa₁₃ polyhedron C₄₈ having topological tetrahedral symmetry.

The fullerenes obtained may be named permutation isomers and be denoted as 1111-loop and 1111-tadpole. Index 1111 indicates that there are four embedded dimers; the words loop and tadpole characterize their position as shown below. It should be emphasized that there are only six possible sites (tetrahedral graph edges). The occupied sites are colored red.

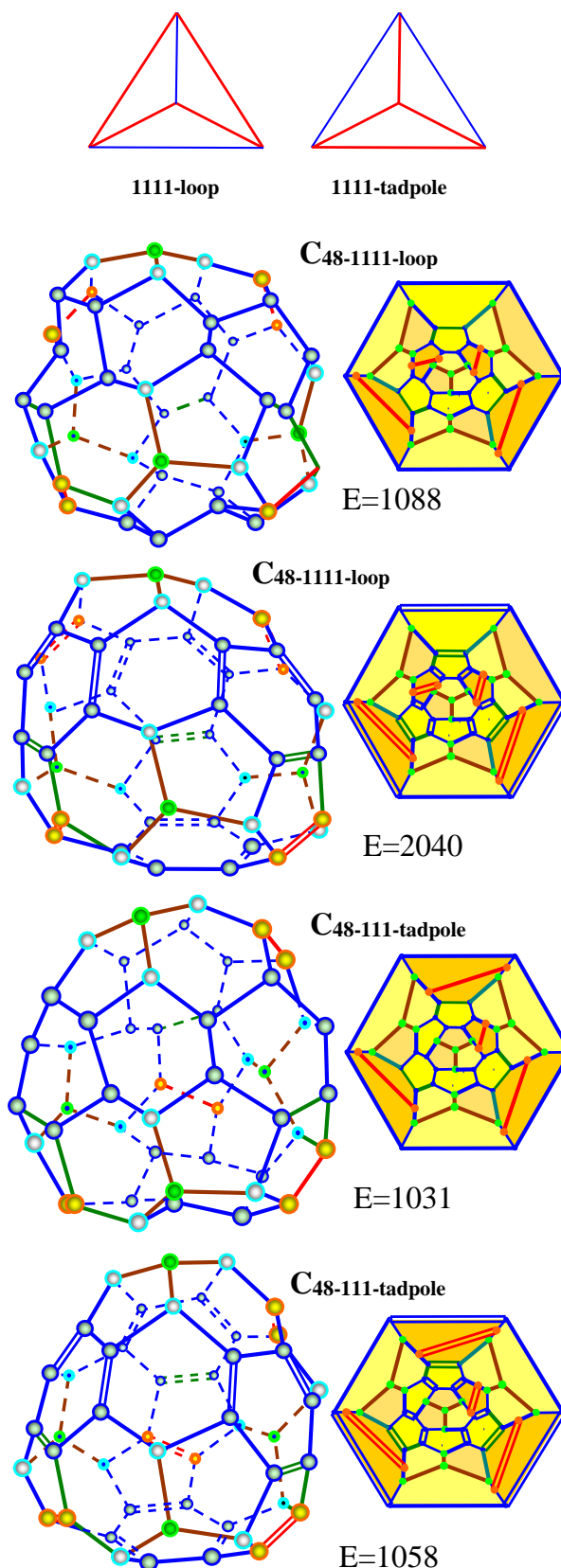


Fig. 39. Two ways of four dimers embedding into perfect fullerene C₄₀ having tetrahedral symmetry: structure, graphs and energy in kJ/mol.

8. DISCUSSION: DIVERSITY

We begin the discussion with the sketchy description of main ideas and notions.

Natural mechanisms of generation. Previously [6] we have systematized possible ways of forming the isomers of midi-fullerenes from C_{30} to C_{40} . We have found that there are three the most natural mechanisms of their formation:

- 1) Embedding carbon dimers into initial fullerenes;
- 2) Fusion of carbon cupolas having the same symmetry;
- 3) Fusion of fullerenes having compatible symmetry.

Just the same mechanisms are valid for the fullerenes in the interval from C_{40} to C_{48} .

Perfect and imperfect fullerenes. In Tables 1 and 2, the calculated energies of fullerene C_{40} are presented for different isomers, the minimum and maximum energies being designated with bold and italic figures, respectively.

From the very beginning we have divided the fullerenes into two groups: the perfect fullerenes of ordinary symmetry and imperfect ones of topological symmetry.

Single and double bonds. In its turn each group contains the fullerenes with single bonds only and with single and double bonds simultaneously; both kinds forming subgroups. We assume that the symmetry of double bonds location about the major axis of cupolas and fullerenes coincides with that of fullerene C_{60} . Using this postulate, we have all the necessary input data for the optimization of the fullerene and cupola structures designed by means of geometric modeling [19] and for subsequent calculation of their energy. The optimized structures of the fullerenes were obtained through the use of Avogadro package [20].

Expected results and customary explanation. Consider at first the energy of C_{40} -fullerene isomers having ordinary symmetry (Table 1). One can see that the energy of single-bonds fullerenes is always less than that of single-

double-bonds ones. It is not strange because the energy of a single bond is 82 kcal and that of a double bond is 147 kcal [21]. In each subgroup the largest energy is attributed to the fullerene of five-fold symmetry containing tetragons (M-fusion). This phenomenon was analyzed in Ref. [22]. The reason is connected with the well-known fact: the more is the curvature of fullerene surface, the more is its distortion energy. In its turn a local curvature is defined by the sum of adjacent angles having a common vertex. The less is the sum, the more is the curvature, and therefore the more is a local stress concentration. The fullerene C_{40} of configuration shown in Fig. 2 (M-fusion) has five tetragons, each of them having four vertices where the angle sum is $90^\circ + 2 \cdot 120^\circ = 330^\circ$. By contrast, the fullerene C_{40} presented in Fig. 3 (RR-fusion) contains ten pentagons, each of them having four vertices where the angle sum is $2 \cdot 108^\circ + 120^\circ = 336^\circ$. Therefore, the second configuration has lesser curvature and so the lesser energy.

Unexpected results. The results of the last two columns of Table 1 deserve detailed consideration. It is known that cluster C_{60} forms at high temperature, so its structure is far removed from that of ideal Buckminster fullerene having I_h icosahedral symmetry [13]. It is assumed that annealing removes defects and reduces the potential energy of the cluster through the use of the Stone-Wales transformation [11].

In our case there are no defects in the initial fullerene C_{40} of C_3 -symmetry (3-6-fold symmetry fusion). Here the Stone-Wales transformation induces only symmetry transition from C_3 to T-symmetry (tetrahedral symmetry). Yet this leads to decreasing the energy for the fullerene with single and double bonds. What is the reason?

Repulsion of valence electron pairs. More than eighty years ago, in 1940 Sidgwick and Powell supposed that the geometry of a forming molecule is dictated by repulsion of valence electron pairs [21,23]. This statement was developed into the system of rules which were named

Table 1. Energy of fullerene C_{40} of ordinary symmetry in kJ/mol.

C_{40}	4-fold 16+24 cupolas fusion	5-fold 20+20 cupolas M-fusion	5-fold 20+20 cupolas RR-fusion	3-6-fold 18+22 cupolas fusion	Stone-Wales transformation (18+22)
E max	2051	<i>3181</i>	1808	1475	1326
E min	1439	<i>1694</i>	1210	946	961
ΔE	612	1487	<i>1538</i>	604	365

Table 2. Energy of fullerene C_{40} of topological symmetry in kJ/mol.

C_{40}	3S-symmetry embedded 1	6-symmetry embedded 11	6-symmetry embedded 101	6-symmetry embedded 1001
E max	1410	<i>2016</i>	1755	1778
E min	1015	921	960	960
ΔE	395	<i>1095</i>	795	818

the theory of repelling valence electron pairs. The main rule is formulated as follows. Electron pairs arrange themselves inside the valence shell of an atom into such configuration which ensures their maximal removing from each other. At that, the electrons pairs behave themselves as if they were repelling each other similar to *point charges*. The assumption is in a good agreement with experimental data for more than 1500 molecules studied. If to present each electron pair as a point and to connect the points by direct lines, one obtains the electronic configuration of chemical bonds [21,23]. Each electronic configuration dictates a definite space molecular structure.

The theory of repelling valent electron pairs was for a long time in the shadow of quantum mechanics. The situation became paradoxical. The repelling theory correctly predicts the shape, but says nothing about the charge value of electron pairs. At the same time, quantum mechanics can predict fairly accurately the energy of a molecule, but strictly speaking says nothing about the shape of a molecule. Here “it is possible to predict the shape of any molecule only by comparison of the energies of different would-be configurations” [21].

Shared and unshared electron pairs. At first, in the theory of repelling valence electron pairs it was supposed that all the electrons pairs, binding and unbinding, are equivalent. Later it turned out that unbinding (unshared) electron pairs have a larger charge than binding (shared) ones [21,24].

Electronic structure of fullerenes. In fullerene C_{26} of C_{3h} -symmetry there are two groups of atoms having different electronic structure: two apex atoms and their three nearest neighbors, and all other ones [5]. The first group of eight atoms consists of sp^3 hybridized atoms; the second one contains sp^2 hybridized atoms. The atoms of the first group have unshared electron pairs.

In the case of the fullerene C_{40} of T-symmetry with single and double bonds, there are four apex sp^3 hybridized atoms (Figs. 6, 7). The other thirty-six atoms are sp^2 hybridized ones as usually accepted. The apex atoms have unshared electron pairs with charge larger than that of other atoms [24].

The optimized molecular structures of the fullerenes obtained by Avogadro package [20] are restricted with the space location of atoms; they do not contain electronic structure. However, knowing the atom positions, one is able to design the electronic structure through the use of the procedure developed in Ref. [25].

In Fig. 40 the electronic configuration of bond charges for fullerene C_{40} of T-symmetry with single and double bonds before and after the Stone-Wales transformation is shown. One can see that here the Stone-Wales transformation is dictated by the repulsion of unshared electron pairs. As a result, the irregular tetrahedron of unshared

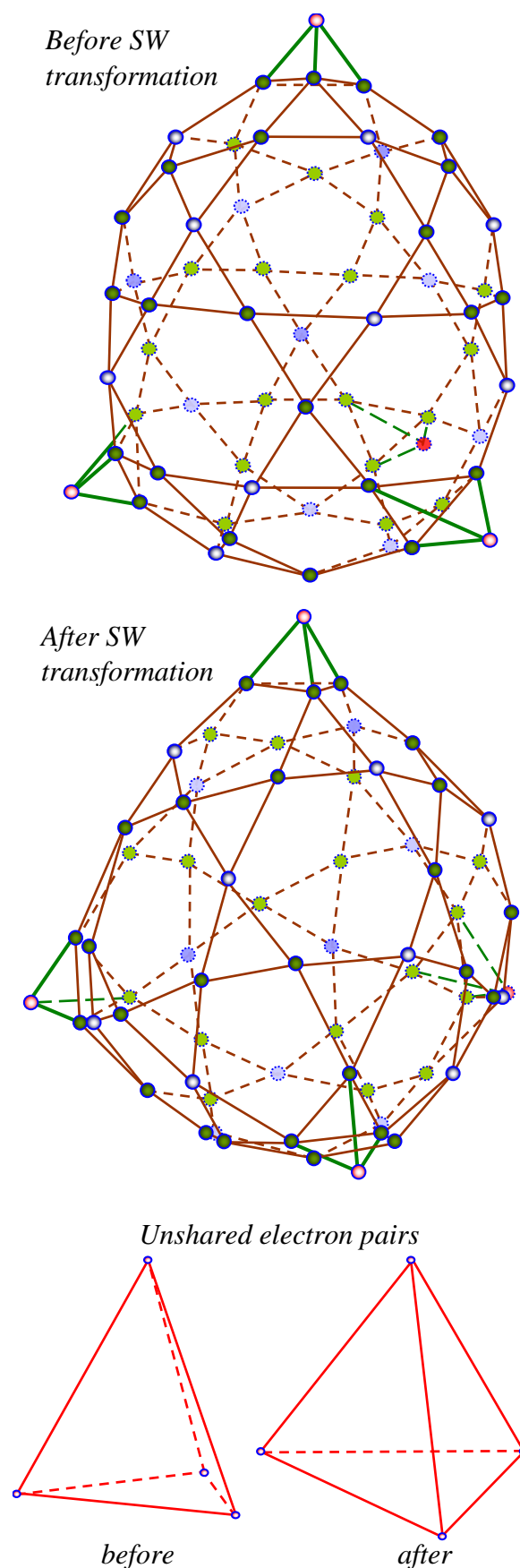


Fig. 40. Electronic structure of fullerene C_{40} before and after Stone-Wales transformation.

electron pairs transforms into the regular tetrahedron with all edges being equal, and that leads to the decreasing of the energy.

However, for the fullerene with only single bonds the result is reverse. What is the reason?

Conformations. It is known that there are three types of molecule motion [26]:

- electron motion relative to atoms;
- periodic changes of the relative locations of nuclei (vibratory motion of molecules);
- periodic orientation changing of a molecule as a whole (rotational motion).

In the last case two parts of a molecule can rotate relative to each other to a large angle. As this takes place, a molecule cannot be considered as a quasi-solid. Contrary to the vibrations of small amplitude near an equilibrium position, the rotary motion realizes itself as a periodic internal movement of large amplitude and small frequency. Here we have at least two minima of the potential energy. The internal rotation plays a key role in forming configurations of chain molecule and macromolecules [27]. Their stable configurations are usually spoken as *conformations*. They are studied for a long time and well known. At the same time the conformations of cyclic hydrocarbon molecules, e.g., cyclohexane, are less known.

Cyclohexane conformations. At first, cyclohexane C_6H_{12} was depicted as a molecule having a plane carbon ring. Later Odd Hassel, the future Nobel Prize winner in chemistry 1969, has shown that this was not true [28]. He has established that cyclohexane had two conformations: in the form of a chair or a boat, the first conformation being predominant [29]. The highly symmetric ‘chair’ configuration belongs to the symmetry group D_{3d} (Fig. 41a). Here [30] four carbon atoms lie in one plane, two others are disposed bilaterally along the plane, all the valence angles CCC are tetrahedral, and all the C–H bonds of neighboring methylene groups are disposed in chess order with respect to each other. From twelve C–H bonds, six bonds are axial and parallel to the symmetry axis of the third order; other six bonds are equatorial. Geometric parameters of the molecule are $r(C-C) = 1.54 \text{ \AA}$. The chair is a stable conformation of cyclohexane. Another conformation is a boat (or a bath) which belongs to the symmetry group C_{2v} (Fig. 41b). It is unstable and at room temperature only one molecule from a thousand has a boat conformation. Chemical and physical methods are unable to fix each conformation separately; they see only an average picture. It is worth noting that similar conformations were observed in semiconductors as static configurations [31].

Conformations and loss of stability. Consider the problem of conformation transitions in the context of the stability theory [32]. To bend a hexagon around any axis of C_6 symmetry, it is necessary to apply forces similar to

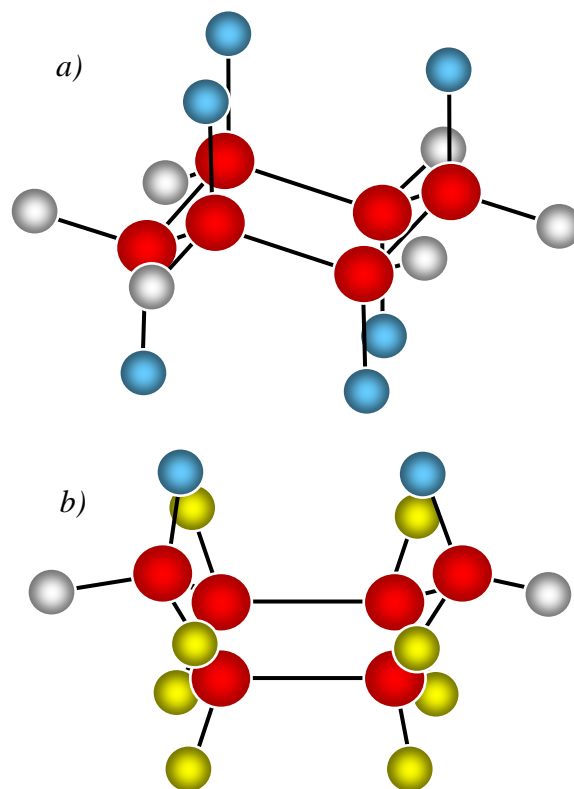


Fig. 41. Structure of a cyclohexane molecule: a) chair conformation, b) boat conformation. Large spheres are carbon atoms, small spheres are hydrogen atoms.

those shown in Fig. 42a. If the bending leads to equilibrium state, one obtains a boat conformation. In terms of the stability theory, it means the stability loss of a first harmonic (mode). One may imagine also the stability loss of a second harmonic (mode) as shown in Fig. 42b. In this case one obtains a chair conformation. The preference depends on elasticity modules and applied forces. The forces arise due to electron pairs interaction as well as due to thermal vibrations of atoms (thermal forces).

One can estimate these forces. According to [24] the bond charges for C–C and C–H bonds are equal to $0.189e$ and $0.077e$, respectively, where e is the electron charge. Consequently, the electrostatic interaction energy for electron pairs of C–C bonds equals $\sim 0.28 \text{ eV}$, whereas the electrostatic interaction energy for electron pairs of C–H bonds is only $\sim 0.03 \text{ eV}$. The thermal motion energy is kT . At $-100 \text{ }^\circ\text{C}$, $300 \text{ }^\circ\text{C}$ and $1200 \text{ }^\circ\text{C}$ it is $\sim 0.014 \text{ eV}$, $\sim 0.05 \text{ eV}$ and $\sim 0.1 \text{ eV}$, respectively. Therefore, at low temperatures, where a molecule has a regular form, this structure is supported by electric forces. At high temperatures, the thermal motion of hydrogen atoms is the main destabilizing factor [29]. This motion changes H–C–H valence angles and, as a consequence, the regular form of a molecule.

Thermal motion is chaotic one. The second mode is more chaotic than the first one, which is highly correlated. Consequently, if the temperature increases, the

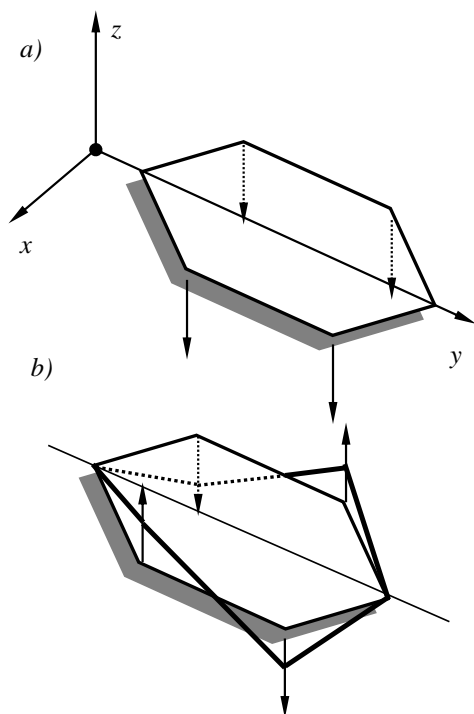


Fig. 42. Stability loss of a hexagon under the action of applied forces.

appearance of the second thermal mode becomes more probable than the first thermal one. In essence, the second mode is torsion [29], and this circumstance gives satisfactory explanation of the conformation transitions.

One of the authors of this paper together with co-workers has found through the use of the new bond-charge molecular dynamics [33,34] that the chair and boat conformations can be formed in fullerene C_{60} at room and higher temperatures [35]. To gain greater insight into this phenomenon, our team has studied conformation transitions in small cyclic hydrocarbon molecules, C_6H_{12} , C_6H_6 , $C_{10}H_8$, $C_{10}H_2$, C_{10} , $C_{13}H_9$ and $C_{14}H_{10}$ [29,35,36]. In addition to other details, it turned out that the circular molecule $C_{13}H_9$ is more rigid and is able to conserve its quasi-plane configuration at low and room temperatures contrary to the linear molecule $C_{14}H_{10}$ that is stable only at low temperatures. It is pertinent to note that the circular molecule has chair conformations whereas the linear molecule has boat ones.

Now consider the unusual results for the 3-6-fold symmetry fullerene with only single bonds and its Stone-Wales transformation (Table 1). Look at the input and output fullerene images on an enlarged scale given by Avogadro package (Fig. 43). We expected that after the Stone-Wales transformation the energy of fullerene will decrease. Contrary to the expectations the effect is reverse. The plausible explanation is as follows.

The structure of fullerenes contains the sequences of hexagons. Close inspection of Fig. 43 shows that the hexagon clusters are different (Fig. 44). The input fullerene has

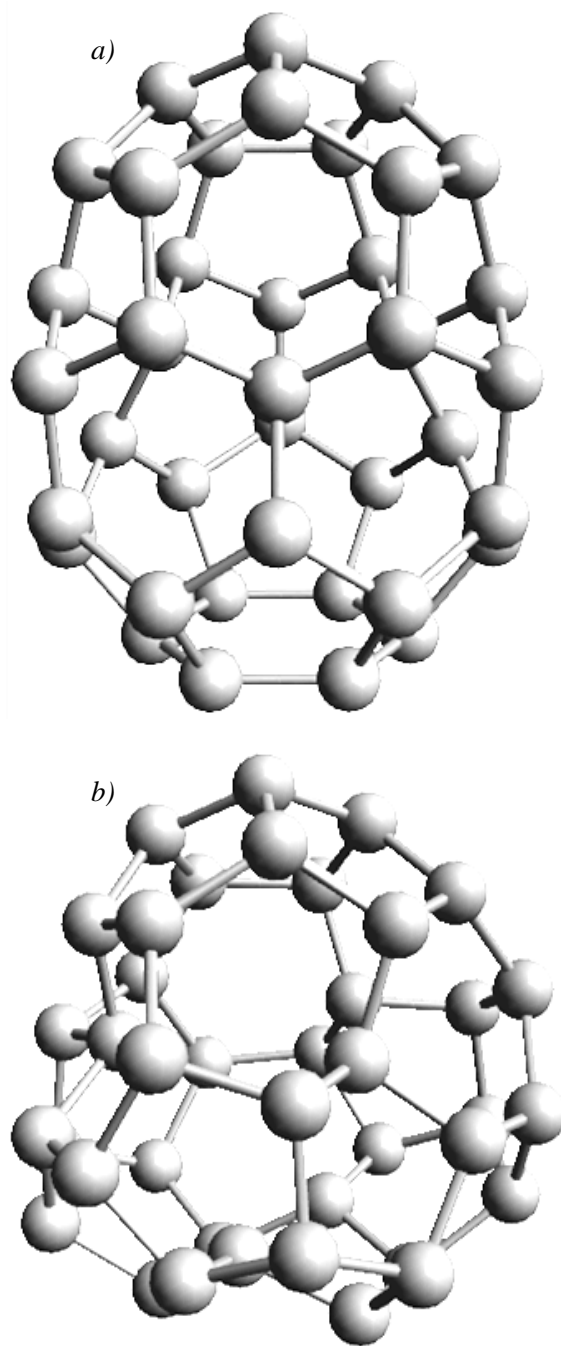


Fig. 43. 3-6-fold symmetry fullerene before (a) and after (b) Stone-Wales transformation.

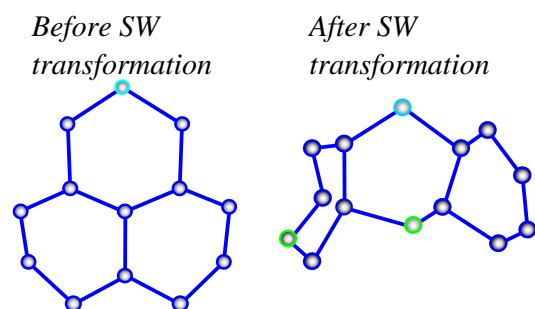


Fig. 44. Hexagon clusters of 3-6-fold symmetry fullerene before and after Stone-Wales transformation.

Table 3. Energy of fullerene C_{42} of topological symmetry in kJ/mol.

C_{42}	3S-sym.	3T-sym.	4-sym.	5-sym.	6-sym. 111	6-sym. 1101	6-sym. 10101	tetrahedral sym.
E max	1256	<i>4253</i>	2519	2755	1894	1866	1960	936
E min	999	<i>2741</i>	1323	1372	933	948	1042	740
ΔE	257	<i>1512</i>	1196	1183	961	918	918	196

Table 4. Energy of fullerene C_{44} of ordinary and topological symmetry in kJ/mol.

C_{44}	3S-sym.	3T-sym.	4-sym. (a)	4-sym. (b)	5-sym. 11	5-sym. 101	6-sym. 1111	6-sym. 11101	6-sym. 11011	tetrahedral sym. 11	tetrahedral sym. 101
E max	1868	<i>4025</i>	2533	2586	2591	2591	2190	1664	2081	980	919
E min	900	<i>2571</i>	1323	1343	1243	1070	1073	1044	976	969	851
ΔE	968	<i>1454</i>	1210	1243	1348	<i>1521</i>	1117	620	1105	11	68

Table 5. Energy of fullerene C_{46} of topological symmetry in kJ/mol.

C_{46}	3S-sym.	3T-sym.	4-sym.	5-sym. 111	5-sym. 1101	6-sym. 11111	tetrahedral sym. 111-ring	tetrahedral sym. 111-cobra	tetrahedral sym. 111-star
E max	1252	<i>3790</i>	2543	2311	1775	1875	980	919	1748
E min	932	<i>2473</i>	1322	1137	1029	1022	969	851	1028
ΔE	320	<i>1317</i>	1221	1174	746	853	11	68	720

Table 6. Energy of fullerene C_{48} of ordinary symmetry in kJ/mol.

C_{48}	3T-sym. fusion	3T-sym. embed.	4-sym. fusion	4-sym. embed.	6M-sym. fusion	6RR-sym. fusion	6-sym. 111 111	6-sym. fusion (fullerenes)
E max	<i>4446</i>	3569	2500	2509	3854	2582	2034	2201
E min	<i>2914</i>	2597	1442	1460	1926	991	991	1291
ΔE	1534	972	1008	949	<i>1928</i>	1491	1043	910

Table 7. Energy of fullerene C_{48} of topological symmetry in kJ/mol.

C_{48}	3S-sym. 11	3S-sym. 101	5 sym. 1111	tetrahedral sym. 1111-loop	tetrahedral sym. 1111-tadpole
E max	1153	1077	<i>2069</i>	2040	1058
E min	1004	940	<i>1141</i>	1088	1031
ΔE	149	137	928	952	27

the clusters which are similar to a circular molecule $C_{13}H_9$, the output one to a linear molecule $C_{14}H_{10}$. In the first case the hexagons have a chair conformation; in the second case they have a boat one. The energy of the boat conformation is a little larger than that of the chair one [24]. This fact explains the result of the Stone-Wales transformation.

Now consider the energy of C_{40} -fullerene isomers of topological symmetry (Table 2). We see that, as before, the energy of single-bond fullerenes is always lower than the energy of single-double-bond ones. It is because the energy of a single bond is lower than that of a double bond. In the E max series the lowest energy is attributed to the fullerene of three-fold S-symmetry containing only one embedded dimer. The highest energy refers to the fullerene of six-fold symmetry with two dimers being the nearest neighbors. It seems that this phenomenon, as before, is connected with different curvature of fullerene surface. In

the E min series variations of energy may be attributed to the conformations of hexagons which create “unsmoothness” energy. The more is the number of chair conformations, the lower is the energy.

9. DISCUSSION: GENERAL FEATURES

We have discussed the peculiar properties of different isomers of fullerene C_{40} . Now consider what the isomers of other fullerenes have in common. Their calculated energies are presented in Tables 3–7, as before, the minimum and maximum energies being designated with bold and italic figures, respectively.

From Tables 3–6 we observe that 3-fold T-symmetry fullerenes C_{42} , C_{44} , C_{46} and C_{48} have the highest energy. The reason is connected with the *local curvature effect* considered above. All the fullerenes of this symmetry have

two trigons, each of them having three vertices where the angle sum is $60^\circ + 2 \cdot 120^\circ = 300^\circ$. The smaller the sum, the greater the curvature, and therefore the greater the local stress concentration and the general energy. This effect does not depend on whether the fullerene has both single and double bonds or only single bonds.

From Tables 3–7 we also see that fullerenes of tetrahedral symmetry C_{42} , C_{44} , C_{46} and C_{48} with single and double bonds have the lowest energy. This phenomenon fits well with the main principle of geometric modeling [19] “the minimum surface at the maximum volume”. This tendency is breaking down for the fullerenes with single bonds only, beginning with fullerene C_{46} . The reason is the “unsmoothness effect” considered above. The more dimers are embedded, the closer the fullerene surface to a sphere. However, the hexagons of different isomers take the conformation which depends on the surroundings. At the same time, since the difference between the energies of boat and chair conformation is small [24], the final energies are close to each other. Indeed, the energies of the isomers of fullerene C_{46} , having the 5-fold symmetry 1101, 6-fold symmetry 11111, tetrahedral symmetry 111 ring, cobra and star, are 1029, 1022, 1070, 1042 and 1028 kJ/mol. The difference is insignificant.

10. CONCLUSION

We have designed possible structures of the isomers of midi-fullerenes, namely C_{40} , C_{42} , C_{44} , C_{46} and C_{48} . Three the most natural mechanisms of their formation were used: fusion of carbon cupolas having the same symmetry, fusion of fullerenes having compatible symmetry and embedding carbon dimers into initial fullerenes. The energies of the fullerenes were calculated through the use of the molecular mechanics package “Avogadro”, being presented together with their graphs. It is found that in the majority of cases the minimum-energy fullerenes are those, which have tetrahedral symmetries. The maximum-energy fullerenes refer to the three-fold T-symmetry.

It should be emphasized that both molecular mechanics and molecular dynamics uses the empirical potentials which incorporate not only direct interatomic interactions but a lot of indirect ones [37–40]. The potentials do not contain electron characteristics of a system in an explicit form; instead, one forgets nuclei, electrons, ions and says about atoms and their interactions [41]. Such averaging requires knowledge of force constants specific for the certain chemical environments. Because of its variety, the number of force constants becomes very large. Nevertheless, such approach allows obtain the shape and energy of molecules, including fullerenes.

To obtain does not denote to understand. The effort to integrate the strong parts of molecular dynamics with the

Sidgwick-Powell theory was done in Ref. [33]. It is assumed that the Sidgwick-Powell point charges can be considered as oscillators. In other words, one can think of a bond-charge as a dynamical variable to some extent independent of its own bond. In this case each bond-charge plays the role of an external field with respect to other bond-charges and these fields polarize the bond. Imagining each bond-charge as a harmonic oscillator, it is possible to write down two systems of the motion equations: one, as before, for atoms and another, new, for electrons, the two systems being dependent on each other [42,43]. Such approach drastically decreases the number of input parameters which are necessary for solving the problem of molecular structures. It should be emphasized that input parameters (force constants) can be calculated on the basis of the electronic theory of molecule vibrations [24] using a small quantity of spectroscopic data. This new molecular dynamics [42,43] has different names: bond-charge molecular dynamics, electronic-molecular dynamics or elerar dynamics.

One of the striking results afforded by elerar dynamics is as follows. In general, the electronic and atomic structures do not coincide; at that, the electronic structure defines the shape of atomic configuration and we have so called hidden symmetry [29]. In this research, for some reasons, the simpler molecular mechanics was used instead of elerar dynamics. However, to gain a more penetrating insight into the results obtained, we were compelled sometimes to return to electronic structure and to use the data which were previously obtained through the use of elerar dynamics.

REFERENCES

- [1] A.I. Melker, M.A. Krupina, *Modeling growth of midi-fullerenes from C_{48} to C_{72}* , *Materials Physics and Mechanics*, 2017, vol. 34, no. 1, pp. 29–36.
- [2] A.I. Melker, M.A. Krupina, R.M. Zarafutdinov, *Fullerenes of the $\Delta N=12$ series*, *Materials Physics and Mechanics*, 2017, vol. 34, no. 1, pp. 46–50.
- [3] A.I. Melker, A.N. Matvienko, *Periodic system of fullerenes: isomers from C_{20} to C_{28}* , in: *Proceedings of NDTCS-2019: Nano-Design, Technology, Computer Simulations*, 2019, pp. 72–78.
- [4] A.M. Kosevich, *Physical Mechanics of Real Crystals*, Naukova Dumka, Kiev, 1981 (in Russian).
- [5] A.I. Melker, M.A. Krupina, R.M. Zarafutdinov, *Fullerenes of the $\Delta N=10$ series*, *Materials Physics and Mechanics*, 2017, vol. 34, no. 1, pp. 37–45.
- [6] A.I. Melker, A.N. Matvienko, M.A. Krupina, *Natural isomers of fullerenes from C_{30} to C_{40}* , *Materials Physics and Mechanics*, 2020, vol. 45, no. 1, pp. 60–78.
- [7] A.I. Melker, T.V. Vorobyeva, *Fusion reactions of cupola half fullerenes*, *St. Petersburg State Polytechnical University Journal: Physics and Mathematics*, 2016, vol. 2, no. 3, pp. 209–216.

- [8] F.J. Sánchez-Barnabe, *Towards a periodic pattern in classical and nonclassical fullerenes with tetrahedral structure*, Materials Physics and Mechanics, 2020, vol. 45, no. 1, pp. 79–85.
- [9] A.I. Melker, A.N. Matvienko, S.A. Starovoitov, *Formation and electronic isomers of tetrahedral fullerene C_{28}* , in: Proceedings of NDTCS-2019: Nano-Design, Technology, Computer Simulations, 2019, pp. 84–87.
- [10] A.J. Stone, D.J. Wales, *Theoretical studies of icosahedral C_{60} and some related species*, Chemical Physics Letters, 1986, vol. 128, no. 5–6, pp. 501–503.
- [11] A.I. Podlivaev, L.A. Openov, *Stone-Wales transformation paths in fullerene C_{60}* , Journal of Experimental and Theoretical Physics Letters, 2005, vol. 81, no. 10, pp. 533–537.
- [12] J. Ma, D. Alfè, A. Michaelides, E. Wang, *Stone-Wales defects in graphene and other planar sp^2 -bonded materials*, Physical Review, 2009, vol. 80, no. 3, art. no. 033407.
- [13] S. Irle, A.J. Page, B. Saha, Y. Wang, K.R.S. Chandrakumar, Y. Nishimoto, H.-J. Qian, K. Morokuma, *Atomistic mechanism of carbon nanostructure self-assembly as predicted by nonequilibrium QM/MD simulations*, in: Practical Aspects of Computational Chemistry II, 2012, Springer, Dordrecht, pp. 103–172.
- [14] M.I. Heggie, G.L. Haffenden, C.D. Lathem, T. Tretvetan, *The Stone-Wales transformation: from fullerenes to graphite, from radiation damage to heat capacity*, Philosophical Transactions of the Royal Society A, 2016, vol. 374, no. 2076, art. no. 20150317.
- [15] A.I. Melker, M.A. Krupina, R.M. Zarafutdinov, *Periodic system of fullerenes: the column of three-fold symmetry*, Nonlinear Phenomena in Complex Systems, 2019, vol. 22, no. 4, pp. 383–394.
- [16] M. Endo, H.W. Kroto, *Formation of carbon nanofibers*, The Journal of Physical Chemistry, 1992, vol. 96, no. 17, pp. 6941–6944.
- [17] A.I. Melker, M.A. Krupina, *Designing mini-fullerenes and their relatives on graph basis*, Materials Physics and Mechanics, 2014, vol. 20, no. 1, pp. 18–24.
- [18] A.I. Melker, M.A. Krupina, A.N. Matvienko, *Nucleation and growth of fullerenes and nanotubes having four-fold symmetry*, Materials Physics and Mechanics, 2021, vol. 47, no. 1, pp. 315–343.
- [19] A.I. Melker, M.A. Krupina, *Geometric modeling of midifullerene growth from C_{32} to C_{48}* , St. Petersburg State Polytechnical University Journal: Physics and Mathematics, 2017, vol. 2, no. 3, pp. 201–208.
- [20] M.D. Hanwell, D.E. Curtis, D.C. Lonie, T. Vandermeersch, E. Zurek, G.R. Hutchison, *Avogadro: an advanced semantic chemical editor, visualization, and analysis platform*, Journal of Cheminformatics, 2012, vol. 4, art. no. 17.
- [21] R.J. Gillespie, *Molecular Geometry*, Van Nostrand Reinhold Co., London, 1972.
- [22] A.I. Melker, M.A. Krupina, *Geometric modeling of midifullerene growth from C_{32} to C_{60}* , St. Petersburg State Polytechnical University Journal: Physics and Mathematics, 2017, vol. 3, no. 1, pp. 22–28.
- [23] N.V. Sidgwick, H.M. Powell, *Bakerian lecture: Stereochemical types and valency groups*, Proceedings of the Royal Society A, vol. 176, no. 965, pp. 153–180.
- [24] A.I. Melker, M.A. Krupina, *Electronic theory of molecule vibrations*, Proceedings of SPIE, 2006, vol. 6253, art. no. 625305.
- [25] A.I. Melker, V. Lonch, *Atomic and electronic structure of mini-fullerenes from four to twenty*, Materials Physics and Mechanics, 2012, vol. 13, no. 1, pp. 22–36.
- [26] M.V. Vol'kenstein, L.A. Gribov, M.A. El'yashevich, B.I. Stepanov, *Vibration of molecules*, Nauka, Moscow, 1972 (in Russian).
- [27] P.J. Flory, *Statistical mechanics of chain molecules*, Interscience Publishers, New York, 1969.
- [28] V. Cholakov, *Nobel prizes*, Mir, Moscow, 1986 (in Russian).
- [29] A.I. Melker, M.A. Krupina, *Hidden symmetry or why cyclic molecules have so strange forms*, Materials Physics and Mechanics, 2010, vol. 9, no. 1, pp. 11–19.
- [30] J.W. Corbett, J.C. Bourgoin, *Defect creation in semiconductors and molecular crystals*, ed. by J.H. Crawford, L.M. Slifkin, Plenum Press, New York, 1975, pp. 1–161.
- [31] A.I. Melker, S.N. Romanov, D.A. Kornilov, *Computer simulation of formation of carbon fullerenes*, Materials Physics and Mechanics, 2000, vol. 2, no. 1, pp. 42–50.
- [32] D.A. Kornilov, A.I. Melker, S.N. Romanov, *New molecular dynamics predicts fullerene formation*, Proceeding of SPIE, 2001, vol. 4348, pp. 146–153.
- [33] D.A. Kornilov, A.I. Melker, S.N. Romanov, *Conformation transition in fullerenes at non-zero temperatures*, Proceeding of SPIE, 2003, vol. 5127, pp. 81–85.
- [34] A.I. Melker, D.A. Kornilov, T.V. Vorobyeva, A. Ivanov, *Conformation transition in cyclohexane and benzol*, Proceeding of SPIE, 2003, vol. 5127, pp. 86–106.
- [35] A.I. Melker, D.A. Kornilov, T.V. Vorobyeva, D. Kalinin, *Conformation transition in naphthalene*, Proceeding of SPIE, 2004, vol. 5400, pp. 112–137.
- [36] A.I. Melker, D.A. Kornilov, T.V. Vorobyeva, A. Ivanov, *Conformation transition in polycyclic molecules $C_{13}H_9$ and $C_{14}H_{10}$* , Proceeding of SPIE, 2004, vol. 5400, pp. 138–159.
- [37] V.V. Barkaline, V.V. Nelayev, A.S. Chashinski, *SiO_2 on CNT: molecular dynamics simulation*, Proceeding of SPIE, 2006, vol. 6253, art. no. 625306.
- [38] A.I. Melker, *Potentials of interatomic interaction in molecular dynamics*, Reviews on Advanced Materials Science, 2009, vol. 20, no. 1, pp. 1–19.
- [39] A.I. Melker, M.A. Vorobyeva (now Krupina), *On the interaction of molecule vibrations*, Reviews on Advanced Materials Science, 2009, vol. 20, no. 1, pp. 14–20.
- [40] V.V. Barkaline, A.S. Chashinski, *Adsorption properties of carbon nanotubes from molecular dynamics viewpoint*, Reviews on Advanced Materials Science, 2009, vol. 20, no. 1, pp. 21–27.
- [41] A.I. Melker, *Dynamics of condensed matter, Part I. Vibrations and waves*, St. Petersburg Academy of Sciences on Strength Problems, St. Petersburg, 2013, 527 p. (in Russian and English).
- [42] A.I. Melker, *Fullerenes and nanotubes: molecular dynamics study*, Proceeding of SPIE, 2004, vol. 5400, pp. 54–64.
- [43] A.I. Melker, *Fiftieth anniversary of molecular dynamics*, Proceeding of SPIE, 2007, vol. 6597, art. no. 659702.

Классификация изомеров фуллеренов от C_{40} до C_{48}

А.И. Мелькер¹, А.Н. Матвиенко², М.А. Крупина³

¹ Санкт-Петербургская академия наук по проблемам прочности, Санкт-Петербургский политехнический университет Петра Великого, ул. Политехническая, 29, 195251, Санкт-Петербург, Россия

² Высшая школа механики и процессов управления, Санкт-Петербургский политехнический университет Петра Великого, ул. Политехническая, 29, 195251, Санкт-Петербург, Россия

³ Кафедра физики, Санкт-Петербургский политехнический университет Петра Великого, ул. Политехническая, 29, 195251, Санкт-Петербург, Россия

Аннотация. Мы сконструировали возможные структуры миди-фуллеренов, а именно C_{40} , C_{42} , C_{44} , C_{46} и C_{48} , используя три наиболее естественных механизма их образования: слияние углеродных куполообразных полуфуллеренов одной и той же симметрии, слияние фуллеренов, обладающих совместимой симметрией, и внедрение углеродных димеров в исходный фуллерен. Энергии образовавшихся фуллеренов были вычислены методом молекулярной механики. Они представлены в статье вместе с графами, характеризующими структуру. Обнаружено, что минимальной энергией обладают фуллерены тетраэдрической симметрии, а максимальной – фуллерены с Т-симметрией третьего порядка.

Ключевые слова: изомер; фуллерен; граф; рост; симметрия